



CERN-EP-2017-178
LHCb-PAPER-2017-020
August 14, 2017

Study of $b\bar{b}$ correlations in high energy proton-proton collisions

LHCb collaboration[†]

Abstract

Kinematic correlations for pairs of beauty hadrons, produced in high energy proton-proton collisions, are studied. The data sample used was collected with the LHCb experiment at centre-of-mass energies of 7 and 8 TeV and corresponds to an integrated luminosity of 3 fb^{-1} . The measurement is performed using inclusive $b \rightarrow J/\psi X$ decays in the rapidity range $2 < y^{J/\psi} < 4.5$. The observed correlations are in good agreement with theoretical predictions.

Published in JHEP 1711 (2017) 030

© CERN on behalf of the LHCb collaboration, licence CC-BY-4.0.

[†]Authors are listed at the end of this paper.

1 Introduction

The production of heavy-flavour hadrons in high energy collisions provides important tests for the predictions of quantum chromodynamics (QCD). Open-charm hadron production has been studied in pp collisions at the Large Hadron Collider (LHC) by the LHCb collaboration at centre-of-mass energies $\sqrt{s} = 5, 7$ and 13 TeV [1–3], by the ATLAS collaboration at $\sqrt{s} = 7$ TeV [4] and by the ALICE collaboration at $\sqrt{s} = 2.76$ and 7 TeV [5–8]. In addition, the CDF collaboration has studied the production of open-charm hadrons in $p\bar{p}$ collisions at the Tevatron at $\sqrt{s} = 1.96$ TeV [9, 10]. For beauty hadrons, the production cross-sections in high energy pp and $p\bar{p}$ collisions have been studied by a number of collaborations [11–14]. Most recently, at the LHC, the LHCb collaboration at $\sqrt{s} = 7, 8$ and 13 TeV and the CMS collaboration at $\sqrt{s} = 8$ TeV studied beauty hadron production using semileptonic decays [15, 16], inclusive decays of beauty hadrons into J/ψ mesons [17–19], and exclusive $B^0 \rightarrow J/\psi K(892)^*0$, $B^+ \rightarrow J/\psi K^+$, $B_s^0 \rightarrow J/\psi K^+K^-$ [20–23], $\Lambda_b^0 \rightarrow J/\psi pK^-$ [24, 25] and $B_c^+ \rightarrow J/\psi \pi^+$ [26, 27] decays. The transverse momentum, p_T , and rapidity, y , spectra are found to be in agreement with calculations at next-to-leading order (NLO). These calculations are made using the general-mass variable-flavour-number scheme (GMVFNS) [28–32], POWHEG [33] and fixed-order with next-to-leading-log resummation (FONLL) [34–39]. For B_c^+ mesons, a good agreement in the shapes of the p_T and y spectra is found [27] with calculations based on a complete order- α_s^4 approach [40–43]. However, the inclusive single-heavy-flavour hadron transverse momentum and rapidity spectra have limited sensitivity to the subprocesses of the production mechanism and the size of higher-order QCD corrections.

The kinematic correlations between the heavy quark and antiquark provide additional information and can enable a better understanding of the production mechanism, such as the contribution of the gluon-splitting, flavour-creation and flavour-excitation processes, as well as the role of higher-order corrections. Such correlations have been studied for pairs of open-charm mesons by the CDF collaboration in the central rapidity region $|y| < 1$ [44, 45] and by the LHCb collaboration in the forward rapidity region $2 < y < 4$ [46]. The difference in the azimuthal angle, ϕ , between two reconstructed open-charm mesons shows a strong correlation, which demonstrates the importance of the gluon-splitting mechanism for the production of $c\bar{c}$ events. For charm production in the central rapidity region, the contributions from flavour-creation and flavour-excitation processes have been identified, in addition to that from gluon splitting [44, 45].

The azimuthal and rapidity correlations in $b\bar{b}$ production have been studied by the UA1 [47], D0 [48] and CDF [49–52] collaborations in $p\bar{p}$ collisions at $\sqrt{s} = 0.63, 1.8$ and 1.96 TeV. At the LHC, the first study of $b\bar{b}$ correlations in high energy pp collisions in the central rapidity region has been performed by the CMS collaboration [53]. The collaboration found that none of the available calculations describe the shapes of the differential cross-section well [54, 55]. In particular, the region where the contributions of gluon-splitting processes are expected to be large is not adequately described by any of the predictions from MC@NLO [54], CASCADE [55], PYTHIA 8 [56], or MADGRAPH [57]. Recently, a study of $b\bar{b}$ correlations in pp collisions in the central rapidity region has been performed by the ATLAS collaboration [58] and a good agreement with calculations was obtained. The four-flavour MADGRAPH5 prediction [59] provides the best overall agreement with data, and performs better than the PYTHIA 8 and HERWIG++ [60] generators.

This paper reports the study of $b\bar{b}$ correlations in high energy hadron collisions in the forward rapidity region. The data sample used was collected with the LHCb experiment at centre-of-mass energies of 7 and 8 TeV and corresponds to integrated luminosities of 1 and 2 fb^{-1} , respectively. The beauty hadrons are reconstructed via their inclusive decays into J/ψ mesons, denoted here as $b \rightarrow J/\psi X$ decays, using J/ψ mesons decaying into the $\mu^+\mu^-$ final state. The results are compared with the leading-order (LO) and NLO expectations from PYTHIA [56,61] and POWHEG [62–65], respectively.

2 Detector and simulation

The LHCb detector [66, 67] is a single-arm forward spectrometer covering the pseudorapidity range $2 < \eta < 5$, designed for the study of particles containing b or c quarks. The detector includes a high-precision tracking system consisting of a silicon-strip vertex detector surrounding the pp interaction region [68], a large-area silicon-strip detector located upstream of a dipole magnet with a bending power of about 4 Tm, and three stations of silicon-strip detectors and straw drift tubes placed downstream of the magnet. The tracking system provides a measurement of momentum, p , of charged particles with a relative uncertainty that varies from 0.5% at low momentum to 1.0% at 200 GeV/ c . The minimum distance of a track to a primary vertex (PV), the impact parameter (IP), is measured with a resolution of $(15 + 29/p_T)\text{ }\mu\text{m}$, where p_T is the component of the momentum transverse to the beam, in GeV/ c . Different types of charged hadrons are distinguished using information from two ring-imaging Cherenkov detectors. Photons, electrons and hadrons are identified by a calorimeter system consisting of scintillating-pad and preshower detectors, an electromagnetic calorimeter and a hadronic calorimeter. Muons are identified by a system composed of alternating layers of iron and multiwire proportional chambers [69].

The online event selection is performed by a trigger [70], which consists of a hardware stage, based on information from the calorimeter and muon systems; followed by a software stage, which applies a full event reconstruction. The hardware trigger selects pairs of opposite-sign muon candidates with a requirement that the product of the muon transverse momenta is larger than 1.7 (2.6) GeV^2/c^2 for data collected at $\sqrt{s} = 7$ (8) TeV. The subsequent software trigger is composed of two stages, the first of which performs a partial event reconstruction. A full event reconstruction is then made at the second stage. In the software trigger, the invariant mass of well-reconstructed pairs of oppositely charged muons that form a vertex with good reconstruction quality is required to exceed 2.7 GeV/c^2 and the vertex is required to be significantly displaced from all PVs.

Simulated samples are used to determine the reconstruction and trigger efficiencies. Proton-proton collisions are generated using PYTHIA [56,61] with a specific LHCb configuration [71]. Decays of hadronic particles are described by EVTGEN [72], in which final-state radiation is generated using PHOTOS [73]. The interaction of the generated particles with the detector, and its response, are implemented using the GEANT4 toolkit [74] as described in Ref. [75].

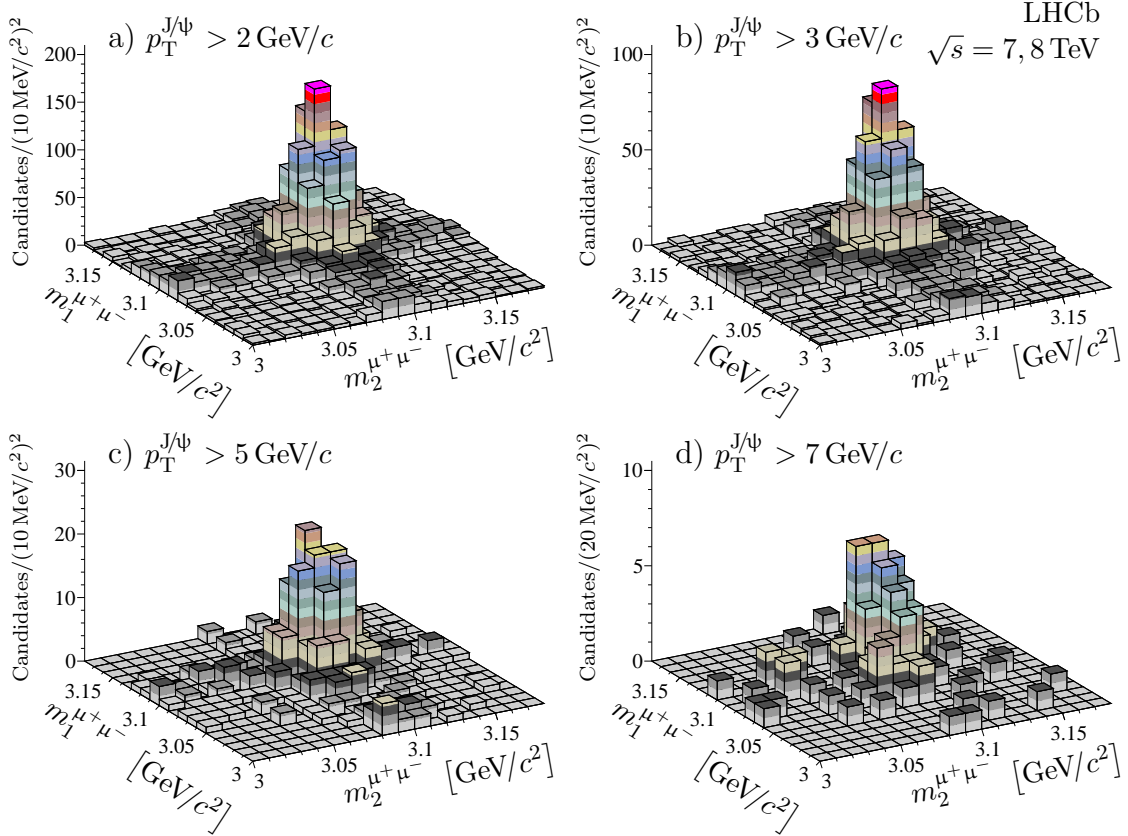


Figure 1: Distribution of $m_1^{\mu^+\mu^-}$ vs $m_2^{\mu^+\mu^-}$ for selected pairs of $J/\psi \rightarrow \mu^+\mu^-$ candidates in different $p_T^{J/\psi}$ regions.

3 Signal selection and efficiency determination

Selected events are required to have two reconstructed $J/\psi \rightarrow \mu^+\mu^-$ candidates. In the following these two candidates are marked with subscripts 1 and 2, which are randomly assigned. The muon candidates must be identified as muons, have good reconstruction quality, $p_T > 500 \text{ MeV}/c$ and $2 < \eta < 5$ [69,76]. Both reconstructed J/ψ candidates are required to have a good-quality vertex, a reconstructed mass in the range $3.00 < m^{\mu^+\mu^-} < 3.18 \text{ GeV}/c^2$, $2 < p_T^{J/\psi} < 25 \text{ GeV}/c$ and $2 < y^{J/\psi} < 4.5$. These criteria ensure a good reconstruction and trigger efficiency. Only events triggered by at least one of the J/ψ candidates are retained. The two J/ψ candidates are required to be associated with the same PV and, in order to suppress background from promptly produced J/ψ mesons, both dimuon vertices are required to be significantly displaced from that PV.

The two-dimensional distribution of the $\mu^+\mu^-$ masses, $m_1^{\mu^+\mu^-}$ and $m_2^{\mu^+\mu^-}$, for the selected pairs of $J/\psi \rightarrow \mu^+\mu^-$ candidates is presented in Fig. 1 for several requirements on $p_T^{J/\psi}$. A clear signal peak, corresponding to events with two J/ψ mesons detached from the PV, is visible.

The signal yield is determined by performing an extended unbinned maximum likelihood

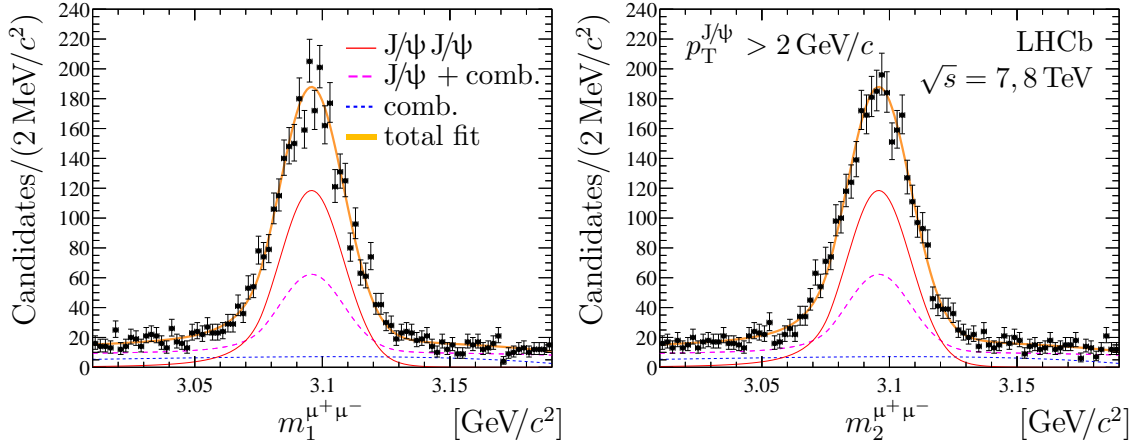


Figure 2: Projections of the extended unbinned maximum likelihood fit to (left) $m_1^{\mu^+\mu^-}$ and (right) $m_2^{\mu^+\mu^-}$ for $p_T^{J/\psi} > 2 \text{ GeV}$. The total fit function is shown as a solid thick orange line. The solid thin red curve shows the signal component, while the background with one true J/ψ candidate is shown by the dashed magenta line and the pure combinatorial background is shown with a dotted thin blue line.

fit to the two-dimensional mass distribution. The distribution is fitted with the function

$$\begin{aligned} \mathfrak{F}(m_1, m_2) &= N_{SS} S(m_1) S(m_2) \\ &+ \frac{N_{SB}}{2} \left(S(m_1) B'(m_2) + B'(m_1) S(m_2) \right) \\ &+ N_{BB} B''(m_1, m_2), \end{aligned}$$

where the first term corresponds to a signal of two J/ψ mesons, the second term corresponds to a combination of one J/ψ meson and combinatorial background; and the last term describes pure combinatorial background. The coefficients N_{SS} , N_{SB} and N_{BB} are the yields for these three components. The signal component, denoted as $S(m)$, is modelled by a double-sided Crystal Ball function [77, 78]. The background component, $B'(m)$, is parameterized as the product of an exponential and a first-order polynomial function and the background component $B''(m_1, m_2)$ is parameterized as the product of two exponential functions $e^{-\tau m_1}$ and $e^{-\tau m_2}$, with the same slope parameter, τ , and a symmetric second-order polynomial. With these parameterizations the overall function is symmetric, $\mathfrak{F}(m_2, m_1) \equiv \mathfrak{F}(m_1, m_2)$. The power-law tail parameters of the double-sided Crystal Ball function are fixed to the values obtained from simulation, leaving the mean and the core width as free parameters. Results of the extended unbinned maximum likelihood fit for the different requirements on $p_T^{J/\psi}$ are presented in Table 1. Figure 2 shows the projections of the fit for $p_T^{J/\psi} > 2 \text{ GeV}$.

Several background sources potentially contribute to the observed J/ψ -pair signal. The first group of sources involves events where two J/ψ mesons originate from different pp collision vertices: it includes events with two J/ψ mesons from decays of beauty hadrons, events with one J/ψ meson originating from a beauty hadron decay and another J/ψ meson produced promptly and, finally, events with two prompt J/ψ mesons. The second group of sources consists of events where both J/ψ mesons originate from the same pp collision, namely prompt J/ψ -pair production [78, 79], and associated production of a prompt J/ψ meson and a $b\bar{b}$ pair, where one of the b hadrons decays into a J/ψ meson.

Table 1: Signal and background yields from the extended unbinned maximum likelihood fit for different requirements on $p_{\text{T}}^{\text{J}/\psi}$. The uncertainties are statistical only.

	$p_{\text{T}}^{\text{J}/\psi} > 2 \text{ GeV}/c$	$p_{\text{T}}^{\text{J}/\psi} > 3 \text{ GeV}/c$	$p_{\text{T}}^{\text{J}/\psi} > 5 \text{ GeV}/c$	$p_{\text{T}}^{\text{J}/\psi} > 7 \text{ GeV}/c$
N_{SS}	2066 ± 72	1092 ± 50	302 ± 17	98 ± 13
N_{SB}	2066 ± 88	949 ± 58	217 ± 17	40 ± 13
N_{BB}	945 ± 73	343 ± 50	39 ± 12	11 ± 9

The contribution from the first group of background sources is estimated from the measured production cross-sections for $b \rightarrow \text{J}/\psi X$ and prompt J/ψ events [17,18], the multiplicity of pp collision vertices and the size of the beam collision region. Taking from simulation an estimate for the probability of reconstructing two spatially close PVs as a single PV, the total relative contribution from these sources is found to be less than 0.1%.

For the second group of background sources, the contribution from prompt J/ψ -pair production is significantly suppressed by the requirement that both dimuon vertices are displaced from the PV. Using the production cross-section for prompt J/ψ pairs¹, the relative contribution from this source is estimated to be less than 0.05%. The background from associated production of $b\bar{b}$ and a prompt J/ψ meson in the same pp collision is calculated assuming double parton scattering is the dominant production mechanism, following Ref. [80]. The relative contribution from this source is estimated to be less than 0.05%.

Normalized differential cross-sections [46,80] are presented as a function of kinematic variables, defined below, and here generically denoted as v ,

$$\frac{1}{\sigma} \frac{d\sigma}{dv} \equiv \frac{1}{N^{\text{cor}}} \frac{\Delta N_i^{\text{cor}}}{\Delta v_i}, \quad (2)$$

where N^{cor} is the total number of efficiency-corrected signal candidates, ΔN_i^{cor} is the number of efficiency-corrected signal candidates in bin i , and Δv_i is the corresponding bin width. The efficiency-corrected yields N^{cor} and ΔN_i^{cor} are calculated as in Refs. [46,81]

$$N^{\text{cor}} = \sum_j \frac{\omega_j}{\epsilon_{\text{tot},j}^{\text{J}/\psi \text{J}/\psi}},$$

$$\Delta N_i^{\text{cor}} = \sum_{j \subset i} \frac{\omega_j}{\epsilon_{\text{tot},j}^{\text{J}/\psi \text{J}/\psi}},$$

where the sum runs over all pairs of J/ψ candidates in the case of N^{cor} and all pairs of J/ψ candidates in bin i in the case of ΔN_i^{cor} . Here $\epsilon_{\text{tot}}^{\text{J}/\psi \text{J}/\psi}$ is the total efficiency for the pair of J/ψ candidates and the weights ω_j are determined using the *sPlot* technique [82].

The total efficiency of the J/ψ pair is estimated on an event-by-event basis as in Refs. [46,78–81]

$$\epsilon_{\text{tot}}^{\text{J}/\psi \text{J}/\psi} = \epsilon_{\text{acc}}^{\text{J}/\psi \text{J}/\psi} \epsilon_{\text{rec\&sel}}^{\text{J}/\psi \text{J}/\psi} \epsilon_{\mu\text{ID}}^{\text{J}/\psi \text{J}/\psi} \epsilon_{\text{trg}}^{\text{J}/\psi \text{J}/\psi}, \quad (3)$$

where ϵ_{acc} is the geometrical acceptance of the LHCb detector, $\epsilon_{\text{rec\&sel}}$ is the reconstruction and selection efficiency for candidates with all final-state muons inside the geometrical

¹ The production cross-section of J/ψ pairs is measured at $\sqrt{s} = 7 \text{ TeV}$ [78]. The cross-section at $\sqrt{s} = 8 \text{ TeV}$ is estimated using a linear interpolation between the measurements at $\sqrt{s} = 7 \text{ TeV}$ and $\sqrt{s} = 13 \text{ TeV}$ [79].

Table 2: Summary of relative systematic uncertainties for the efficiency-corrected signal yield.

Source	Uncertainty [%]
Signal determination	< 1.0
Muon identification	0.4
Track reconstruction	1.7
Trigger	1.2
Simulated sample size	< 0.1

acceptance, $\epsilon_{\mu\text{ID}}$ is the muon identification (μID) efficiency for the selected candidates and ϵ_{trg} is the trigger efficiency for the selected candidates satisfying the μID requirement. The efficiencies, ϵ_{acc} , $\epsilon_{\text{rec\&sel}}$ and $\epsilon_{\mu\text{ID}}$, are factorized as

$$\epsilon^{\text{J}/\psi \text{J}/\psi} \equiv \epsilon^{\text{J}/\psi_1} \epsilon^{\text{J}/\psi_2}, \quad (4)$$

while the trigger efficiency is decomposed as in Refs. [46, 78, 79]

$$\epsilon_{\text{trg}}^{\text{J}/\psi \text{J}/\psi} \equiv 1 - \left(1 - \epsilon_{\text{trg}}^{\text{J}/\psi_1}\right) \left(1 - \epsilon_{\text{trg}}^{\text{J}/\psi_2}\right). \quad (5)$$

The efficiencies $\epsilon_{\text{acc}}^{\text{J}/\psi}$, $\epsilon_{\text{rec\&sel}}^{\text{J}/\psi}$ and $\epsilon_{\text{trg}}^{\text{J}/\psi}$ are estimated as functions of the transverse momentum and rapidity of the J/ψ meson using simulation. The trigger efficiency for single J/ψ mesons, $\epsilon_{\text{trg}}^{\text{J}/\psi}$, has been validated using data. The muon identification efficiency for J/ψ mesons is factorized as

$$\epsilon_{\mu\text{ID}}^{\text{J}/\psi} \equiv \epsilon_{\mu\text{ID}}^{\mu^+} \epsilon_{\mu\text{ID}}^{\mu^-}, \quad (6)$$

where the corresponding single-muon identification efficiency, $\epsilon_{\mu\text{ID}}^{\mu^\pm}$, is determined as a function of muon momentum and pseudorapidity using large samples of prompt J/ψ mesons.

3.1 Systematic uncertainties

The systematic uncertainty due to the imprecise determination of the luminosity does not enter in the normalized differential cross-sections. The systematic uncertainties, related to the evaluation of the efficiency-corrected signal yields N^{cor} and ΔN_i^{cor} from Eq. (2) are summarized in Table 2 and are discussed in detail below.

Systematic uncertainties associated with the signal determination are studied by varying the signal and background shapes used for the fit function. For the signal parameterization, the power-law tail parameters of the double-sided Crystal Ball function are varied according to the results of fits to large samples of low-background $\text{b} \rightarrow \text{J}/\psi \text{X}$ and $\text{B}^+ \rightarrow \text{J}/\psi \text{K}^+$ candidates. The alternative signal shape parameterization from Ref. [83] is also used in the fits. For the parameterization of the background functions, $B'(m)$ and $B''(m_1, m_2)$, the order of the polynomial functions is varied. The difference in the fitted signal yields does not exceed 1% in all of the above cases.

The systematic uncertainty related to the muon identification is estimated to be 0.4%. It is obtained from the uncertainties for the single-particle identification efficiencies, $\epsilon_{\mu\text{ID}}^{\mu^\pm}$, using pseudoexperiments.

The efficiency $\epsilon_{\text{rec\&sel}}^{\text{J}/\psi}$ is corrected on a per-track basis for small discrepancies between data and simulation using data-driven techniques [76, 84]. The uncertainty in the correction

factor is propagated to the determination of the efficiency-corrected signal yields using pseudoexperiments. This results in a systematic uncertainty of 0.6%. Added in quadrature to the (correlated) uncertainty from the track reconstruction of 0.4% per track (1.6% in total) these sources give an overall systematic uncertainty associated with the track reconstruction of 1.7%.

The trigger efficiency has been validated using large low-background samples of $B^+ \rightarrow J/\psi K^+$ decays and inclusive samples of J/ψ mesons. Taking the largest difference between simulation and data for $\epsilon_{\text{trg}}^{J/\psi}$, the corresponding systematic uncertainty for the efficiency-corrected yields is 1.2%.

The uncertainties in the efficiencies $\epsilon_{\text{acc}}^{J/\psi}$, $\epsilon_{\text{rec\&sel}}^{J/\psi}$ and $\epsilon_{\text{trg}}^{J/\psi}$, which are due to the limited size of the simulation samples, are propagated to the efficiency-corrected signal yields using pseudoexperiments and are less than 0.1%.

Part of the uncertainties, summarized in Table 2, cancel in the ratio $\frac{\Delta N_i^{\text{cor}}}{N^{\text{cor}}}$ and thus do not affect the normalized differential cross-sections. For all bins for which the normalized differential cross-sections are evaluated, the systematic uncertainty is much smaller than the corresponding statistical uncertainty and is therefore neglected hereafter.

4 Results

The normalized differential production cross-sections defined by Eq. (2) are presented as a function of the following variables:

- $|\Delta\phi^*|$, the difference in the azimuthal angle, ϕ^* , between the two beauty hadrons, where ϕ^* is estimated from the direction of the vector from the PV to the decay vertex of the J/ψ meson;
- $|\Delta\eta^*|$, the difference in the pseudorapidity, η^* , between the two beauty hadrons, where η^* is estimated from the direction of the vector from the PV to the decay vertex of the J/ψ meson;
- $\mathcal{A}_T \equiv \left| \frac{p_T^{J/\psi_1} - p_T^{J/\psi_2}}{p_T^{J/\psi_1} + p_T^{J/\psi_2}} \right|$, the asymmetry between the transverse momenta of two J/ψ mesons;
- $m^{J/\psi J/\psi}$, the mass of the J/ψ pair;
- $p_T^{J/\psi J/\psi}$, the transverse momentum of the J/ψ pair;
- $y^{J/\psi J/\psi}$, the rapidity of the J/ψ pair.

The differential cross-sections with respect to other variables are given in Appendix A. The shapes for the differential production cross-sections for $|\Delta\phi^*|$ and $|\Delta\eta^*|$ variables are independent of the decay of the long-lived beauty hadrons and directly probe the production properties of pairs of beauty hadrons. The other variables have a minor dependence both on the branching fractions of different beauty hadrons, as well as on the $b \rightarrow J/\psi X$ decay kinematics.

The normalized differential production cross-sections are shown in Figs. 3, 4, 5 and 6 for different requirements on the minimum transverse momentum of the J/ψ mesons. Since the distributions obtained for data accumulated at $\sqrt{s} = 7$ and 8 TeV are very similar,

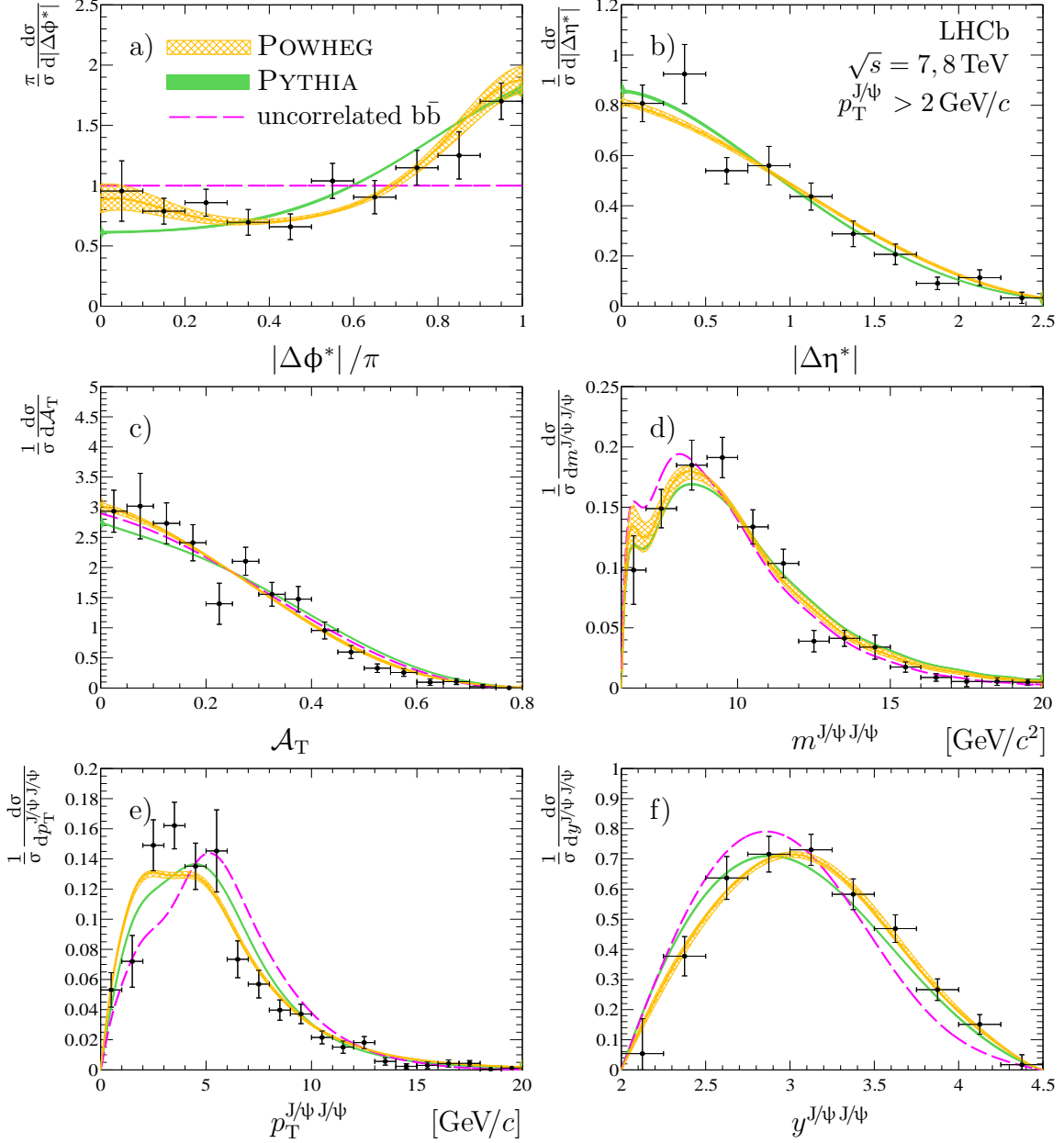


Figure 3: Normalized differential production cross-sections (points with error bars) for a) $|\Delta\phi^*|/\pi$, b) $|\Delta\eta^*|$, c) \mathcal{A}_T , d) $m^{J/\psi J/\psi}$, e) $p_T^{J/\psi J/\psi}$ and f) $y^{J/\psi J/\psi}$ together with the POWHEG (orange line) and PYTHIA (green band) predictions. The expectations for uncorrelated $b\bar{b}$ production are shown by the dashed magenta line. The uncertainties in the POWHEG and PYTHIA predictions due to the choice of factorization and renormalization scales are shown as orange cross-hatched and green solid areas, respectively.

they are treated together. In general, the width of the resolution function is much smaller than the bin width, *i.e.* the results are not affected by bin-to-bin migration. The exception to this is a small fraction of events with $2.0 < p_T^{J/\psi} < 2.5$ GeV/ c , where the resolution for $|\Delta\phi^*|$ and $|\Delta\eta^*|$ is close to half of the bin-width.

The normalized differential production cross-sections are compared with expectations from POWHEG [62–65] and PYTHIA [56, 61, 71] using the parton distribution functions

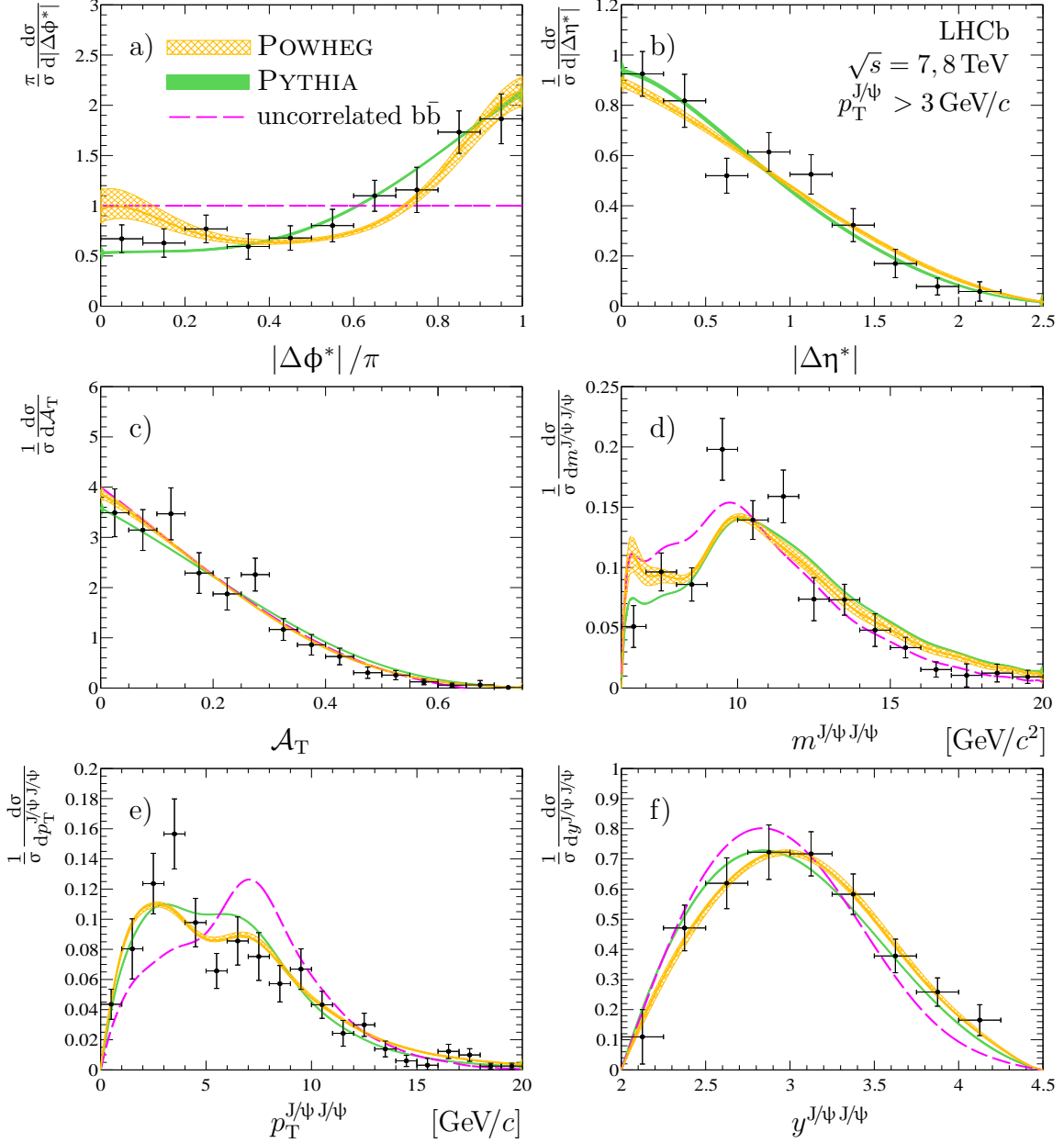


Figure 4: Normalized differential production cross-sections (points with error bars) for a) $|\Delta\Phi^*|/\pi$, b) $|\Delta\eta^*|$, c) \mathcal{A}_T , d) $m^{J/\psi J/\psi}$, e) $p_T^{J/\psi J/\psi}$ and f) $y^{J/\psi J/\psi}$ together with the POWHEG (orange line) and PYTHIA (green band) predictions. The expectations for uncorrelated $b\bar{b}$ production are shown by the dashed magenta line. The uncertainties in the POWHEG and PYTHIA predictions due to the choice of factorization and renormalization scales are shown as cross-hatched and green solid areas, respectively.

from CT09MCS [85], CTEQ6L1 [86] and CTEQ6.6 [87] for the samples produced with POWHEG, PYTHIA 6 and PYTHIA 8, respectively. Since no visible difference between PYTHIA 6 and PYTHIA 8 samples are found, they are combined. For the POWHEG samples the default configuration is used except for the b-quark mass, which is set to $4.75 \text{ GeV}/c^2$. To illustrate the size of the correlations between the two b quarks, predictions from an artificial data-driven model of uncorrelated $b\bar{b}$ production are also presented. This model

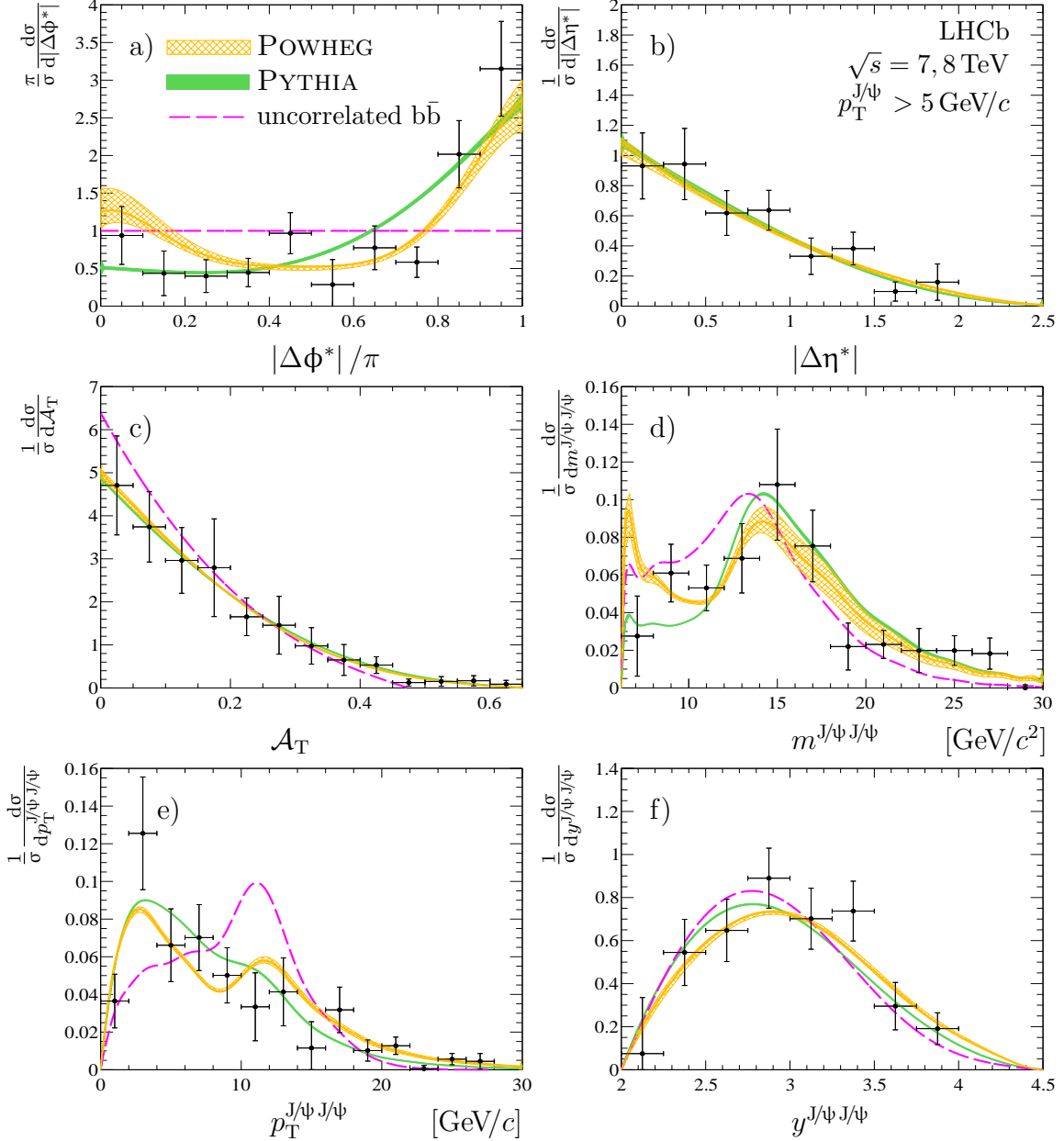


Figure 5: Normalized differential production cross-sections (points with error bars) for a) $|\Delta\Phi^*|/\pi$, b) $|\Delta\eta^*|$, c) \mathcal{A}_T , d) $m^{J/\psi J/\psi}$, e) $p_T^{J/\psi J/\psi}$ and f) $y^{J/\psi J/\psi}$ together with the POWHEG (orange line) and PYTHIA (green band) predictions. The expectations for uncorrelated $b\bar{b}$ production are shown by the dashed magenta line. The uncertainties in the POWHEG and PYTHIA predictions due to the choice of factorization and renormalization scales are shown as orange cross-hatched and green solid areas, respectively.

is based on the measured transverse momenta and rapidity spectra for $b \rightarrow J/\psi X$ decays [17, 18], assuming uncorrelated production of b and \bar{b} quarks. The momenta of the two J/ψ mesons are sampled according to the measured $(p_T^{J/\psi}, y^{J/\psi})$ spectra, assuming a uniform distribution in the azimuthal angle, $\phi^{J/\psi}$. This allows the distributions for all variables except for $|\Delta\eta^*|$ to be predicted. This model is considered as an extreme case that corresponds to uncorrelated $b\bar{b}$ production; in contrast, the leading-order collinear

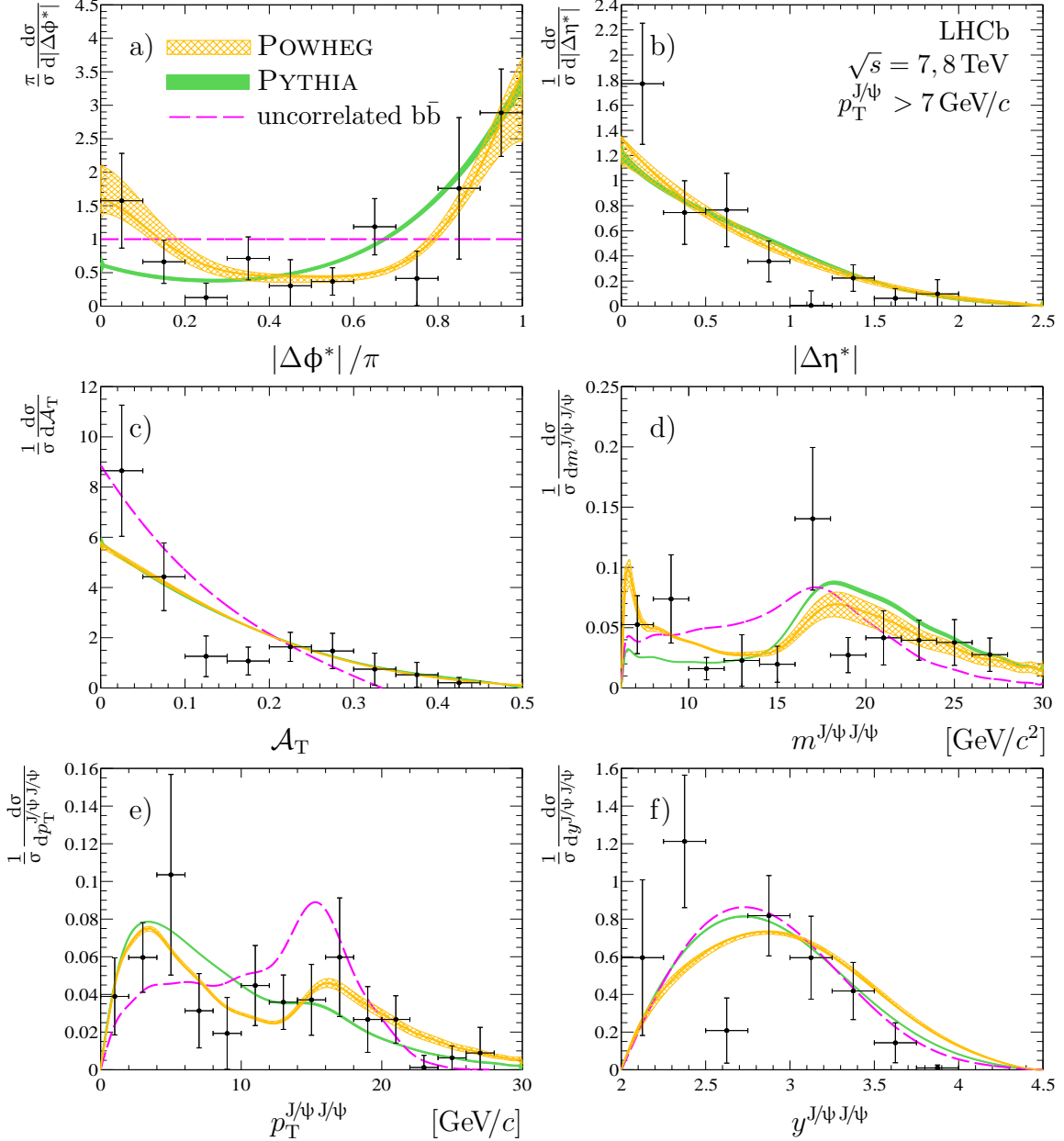


Figure 6: Normalized differential production cross-sections (points with error bars) for a) $|\Delta\Phi^*|/\pi$, b) $|\Delta\eta^*|$, c) \mathcal{A}_T , d) $m^{J/\psi J/\psi}$, e) $p_T^{J/\psi J/\psi}$ and f) $y^{J/\psi J/\psi}$ together with the POWHEG (orange line) and PYTHIA (green band) predictions. The expectations for uncorrelated $b\bar{b}$ production are shown by the dashed magenta line. The uncertainties in the POWHEG and PYTHIA predictions due to the choice of factorization and renormalization scales are shown as orange cross-hatched and green solid areas, respectively.

approximation, where the transverse momentum of the $b\bar{b}$ system from the $gg \rightarrow b\bar{b}$ process is zero, results in maximum correlation. The smearing of the transverse momenta of the initial gluons could result in significant decorrelations of the initially highly correlated heavy-flavour quarks. It should be noted that the model using uncorrelated $b\bar{b}$ pairs also mimics a possible small contribution of double parton scattering to $b\bar{b}$ pair production.

In general, both POWHEG and PYTHIA describe the data well for all distributions,

suggesting that NLO effects in $b\bar{b}$ production in the studied kinematic region are small compared with the experimental precision. Unlike the measurements with open-charm mesons [44–46], no significant contribution from gluon splitting is observed at small $|\Delta\phi^*|$. This observation is in agreement with expectations, since the contribution from gluon splitting is suppressed due to the large mass of the beauty quark. For $p_T^{J/\psi} > 5$ and 7 GeV, there is a hint of a small enhancement at small $|\Delta\phi^*|$. This also agrees with the expectation of a larger contribution of gluon splitting at higher p_T . Another large enhancement towards the threshold in $m^{J/\psi J/\psi}$ is predicted by POWHEG for $p_T^{J/\psi} > 5$ and 7 GeV, due to large leading-logarithm corrections [88]. No evidence for this enhancement is observed in the LHCb data, as can be seen in Figs. 5d and 6d. The data agree well with the model of uncorrelated $b\bar{b}$ production for $y^{J/\psi J/\psi}$ and \mathcal{A}_T , and also for $p_T^{J/\psi J/\psi}$ and $m^{J/\psi J/\psi}$ in the $p_T^{J/\psi} > 2$ GeV/ c region. This suggests gluon emission from the initial and/or final state, or large effective smearing of the transverse momenta of the gluons, $\mathcal{O}(3$ GeV/ c), resulting in large decorrelation of the produced heavy quarks.

5 Summary and conclusions

Kinematic correlations for pairs of beauty hadrons, produced in high energy proton-proton collisions, are studied. The data sample used was collected with the LHCb experiment at centre-of-mass energies of 7 and 8 TeV and corresponds to an integrated luminosity of 3 fb $^{-1}$. The measurement is performed using $b \rightarrow J/\psi X$ decays in the kinematic range $2 < y^{J/\psi} < 4.5$, $2 < p_T^{J/\psi} < 25$ GeV/ c . The observed correlations agree with PYTHIA (LO) and POWHEG (NLO) predictions, suggesting NLO effects in $b\bar{b}$ production are small. In particular, no large contribution from gluon splitting is observed. The present data do not allow discrimination of theory predictions in the region of large p_T of the J/ψ mesons, where the difference between POWHEG and PYTHIA predictions is larger. Such discrimination will be possible with future measurements with larger data samples at higher energy.

Acknowledgements

We would like to thank P. Nason and A.K. Likhoded for interesting and stimulating discussions on production of heavy-flavours. We express our gratitude to our colleagues in the CERN accelerator departments for the excellent performance of the LHC. We thank the technical and administrative staff at the LHCb institutes. We acknowledge support from CERN and from the national agencies: CAPES, CNPq, FAPERJ and FINEP (Brazil); MOST and NSFC (China); CNRS/IN2P3 (France); BMBF, DFG and MPG (Germany); INFN (Italy); NWO (The Netherlands); MNiSW and NCN (Poland); MEN/IFA (Romania); MinES and FASO (Russia); MinECo (Spain); SNSF and SER (Switzerland); NASU (Ukraine); STFC (United Kingdom); NSF (USA). We acknowledge the computing resources that are provided by CERN, IN2P3 (France), KIT and DESY (Germany), INFN (Italy), SURF (The Netherlands), PIC (Spain), GridPP (United Kingdom), RRCKI and Yandex LLC (Russia), CSCS (Switzerland), IFIN-HH (Romania), CBPF (Brazil), PL-GRID (Poland) and OSC (USA). We are indebted to the communities behind the multiple open source software packages on which

we depend. Individual groups or members have received support from AvH Foundation (Germany), EPLANET, Marie Skłodowska-Curie Actions and ERC (European Union), ANR, Labex P2IO, ENIGMASS and OCEVU, and Région Auvergne-Rhône-Alpes (France), RFBR and Yandex LLC (Russia), GVA, XuntaGal and GENCAT (Spain), Herchel Smith Fund, the Royal Society, the English-Speaking Union and the Leverhulme Trust (United Kingdom).

Appendices

A Additional variables

In this appendix the normalized differential production cross-sections are studied for additional variables, namely

- $|\Delta\phi^{J/\psi}|$, the difference in the azimuthal angle $\phi^{J/\psi}$ between the momentum directions of two J/ψ mesons;
- $|\Delta\eta^{J/\psi}|$, the difference in the pseudorapidity $\eta^{J/\psi}$ between the momentum directions of two J/ψ mesons;
- $|\Delta y^{J/\psi}|$, the difference in the rapidity $y^{J/\psi}$ between the two J/ψ mesons.

Unlike $|\Delta\phi^*|/\pi$ and $|\Delta\eta^*|$, which are largely independent on the decays of beauty hadrons, all these variables have a minor dependence both on the branching fractions of different beauty hadrons, as well as on the $b \rightarrow J/\psi X$ decay kinematics.

The corresponding differential cross-sections are presented in Figs. 7 and 8. They are compared with expectations from the POWHEG [62–65] and PYTHIA [56, 61, 71] generators and with expectations from the data-driven model of uncorrelated $b\bar{b}$ production, described in Sect. 4. Also in this case both POWHEG and PYTHIA describe the data well for all distributions, suggesting a small role of next-to-leading order effects in $b\bar{b}$ production in the studied kinematical range compared to the experimental precision. The data agree well with the model of uncorrelated $b\bar{b}$ production for $|\Delta\eta^{J/\psi}|$ and $|\Delta y^{J/\psi}|$, supporting the hypothesis of large effective decorrelation of the produced heavy quarks.

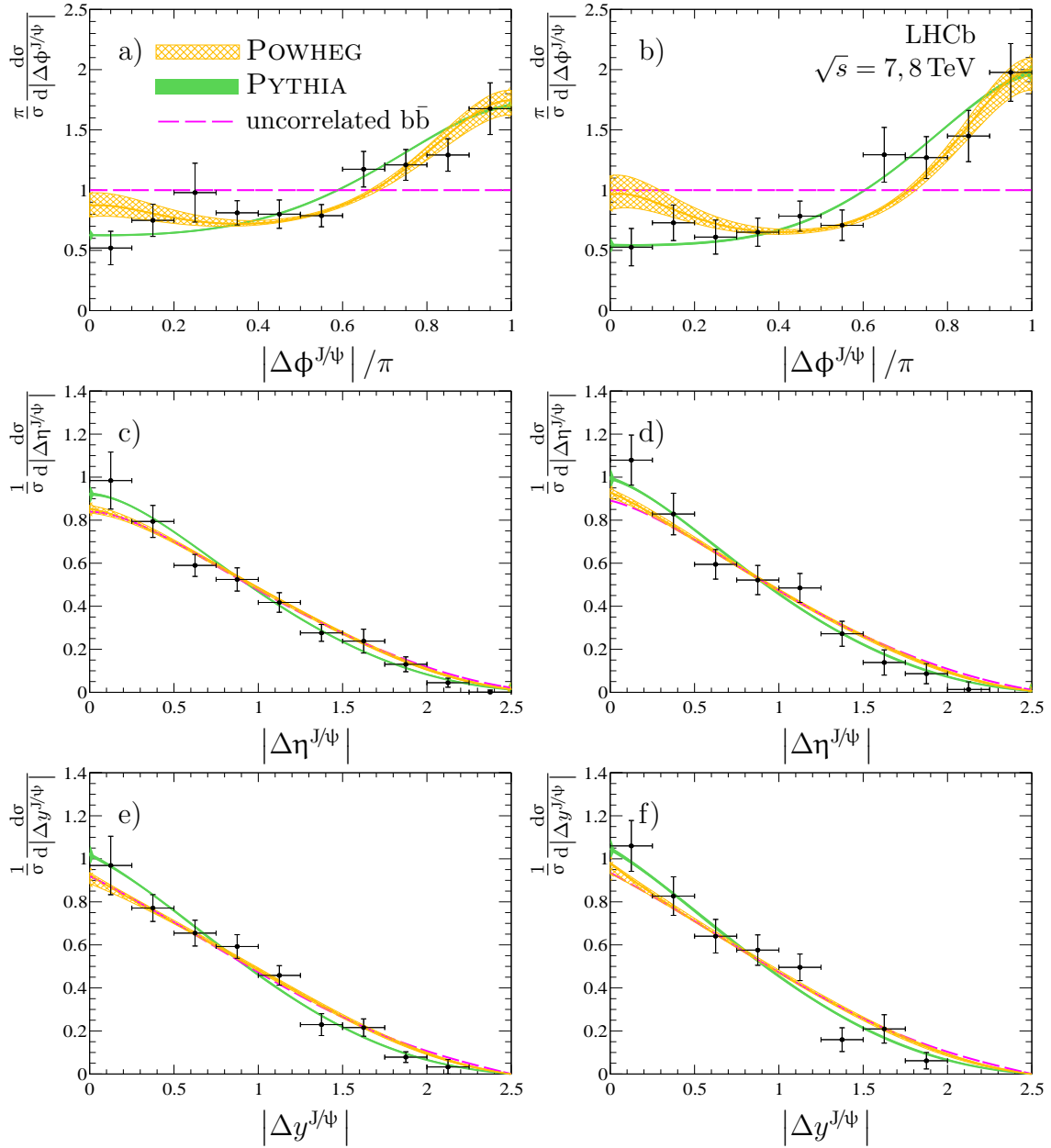


Figure 7: Normalized differential production cross-sections (points with error bars) for $p_T^{J/\psi} > 2 \text{ GeV}/c$ (left) and $p_T^{J/\psi} > 3 \text{ GeV}/c$ (right) data for a,b) $|\Delta\phi^{J/\psi}|/\pi$, c,d) $|\Delta\eta^{J/\psi}|$, and e,f) $|\Delta y^{J/\psi}|$, together with the POWHEG (orange line) and PYTHIA (green band) predictions. The expectations for uncorrelated $b\bar{b}$ production are shown by the dashed magenta line. The uncertainties in the POWHEG and PYTHIA predictions due to the choice of factorization and renormalization scales are shown as orange cross-hatched and green solid areas, respectively.

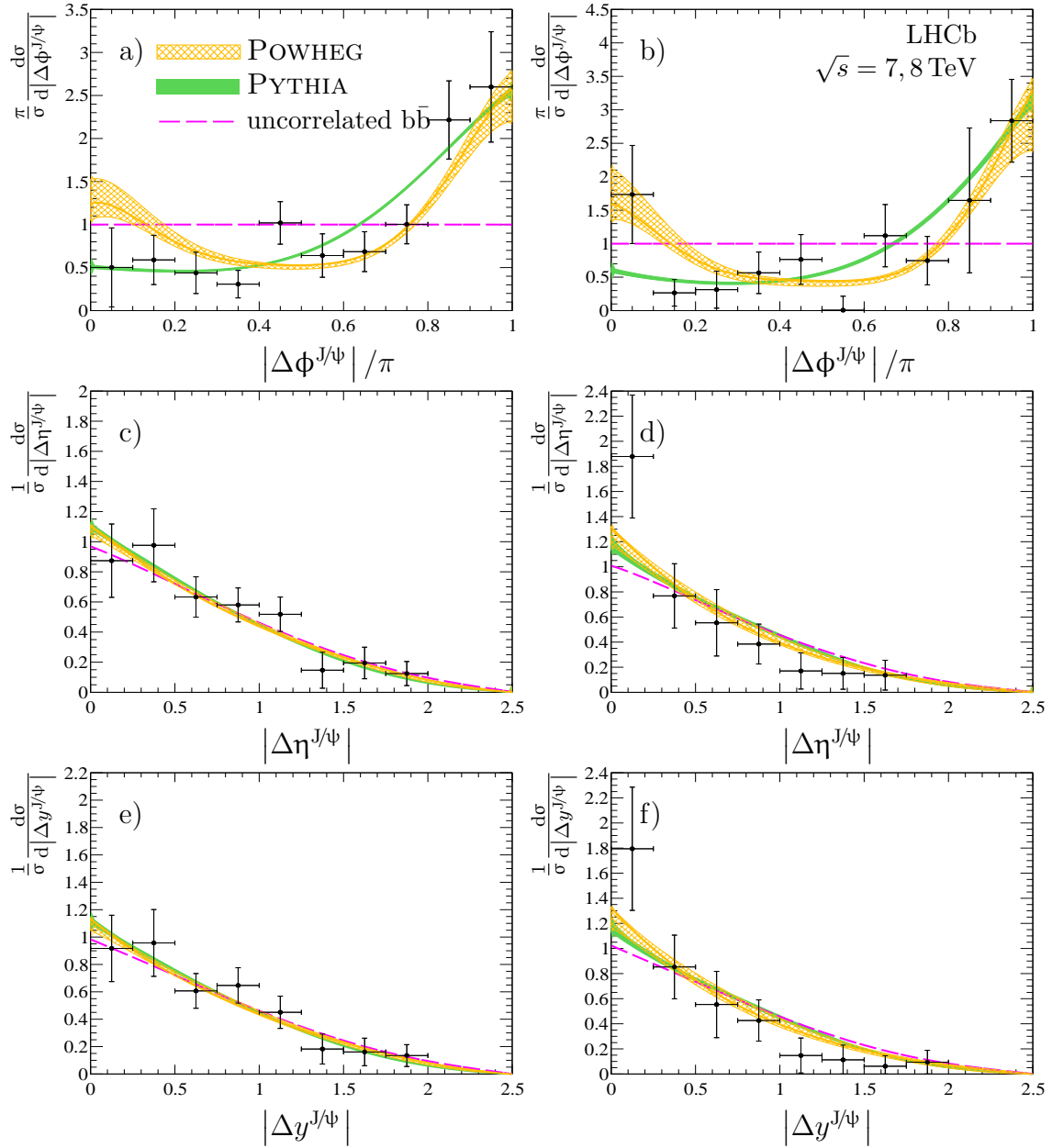


Figure 8: Normalized differential production cross-sections (points with error bars) for $p_T^{J/\psi} > 5 \text{ GeV}/c$ (left) and $p_T^{J/\psi} > 7 \text{ GeV}/c$ (right) data for a,b) $|\Delta\phi^{J/\psi}|/\pi$, c,d) $|\Delta\eta^{J/\psi}|$, and e,f) $|\Delta y^{J/\psi}|$, together with the POWHEG (orange line) and PYTHIA (green band) predictions. The expectations for uncorrelated $b\bar{b}$ production are shown by the dashed magenta line. The uncertainties in the POWHEG and PYTHIA predictions due to the choice of factorization and renormalization scales are shown as orange cross-hatched and green solid areas, respectively.

References

- [1] LHCb collaboration, R. Aaij *et al.*, *Measurements of prompt charm production cross-sections in pp collisions at $\sqrt{s} = 5$ TeV*, JHEP **06** (2017) 147, arXiv:1610.02230.
- [2] LHCb collaboration, R. Aaij *et al.*, *Prompt charm production in pp collisions at $\sqrt{s} = 7$ TeV*, Nucl. Phys. **B871** (2013) 1, arXiv:1302.2864.
- [3] LHCb collaboration, R. Aaij *et al.*, *Measurements of prompt charm production cross-sections in pp collisions at $\sqrt{s} = 13$ TeV*, JHEP **03** (2016) 159, Erratum *ibid.* **09** (2016) 013, Erratum *ibid.* **05** (2017) 074, arXiv:1510.01707.
- [4] ATLAS collaboration, G. Aad *et al.*, *Measurement of $D^{*\pm}$, D^\pm and D_s^\pm meson production cross sections in pp collisions at $\sqrt{s} = 7$ TeV with the ATLAS detector*, Nucl. Phys. **B907** (2016) 717, arXiv:1512.02913.
- [5] ALICE collaboration, B. Abelev *et al.*, *Measurement of charm production at central rapidity in proton-proton collisions at $\sqrt{s} = 2.76$ TeV*, JHEP **07** (2012) 191, arXiv:1205.4007.
- [6] ALICE collaboration, B. Abelev *et al.*, *Measurement of charm production at central rapidity in proton-proton collisions at $\sqrt{s} = 7$ TeV*, JHEP **01** (2012) 128, arXiv:1111.1553.
- [7] ALICE collaboration, B. Abelev *et al.*, *D_s^+ meson production at central rapidity in proton-proton collisions at $\sqrt{s} = 7$ TeV*, Phys. Lett. **B718** (2012) 279, arXiv:1208.1948.
- [8] ALICE collaboration, J. Adam *et al.*, *D-meson production in p-Pb collisions at $\sqrt{s_{NN}} = 5.02$ TeV and in pp collisions at $\sqrt{s} = 7$ TeV*, Phys. Rev. **C94** (2016) 054908, arXiv:1605.07569.
- [9] CDF collaboration, D. Acosta *et al.*, *Measurement of prompt charm meson production cross sections in $p\bar{p}$ collisions at $\sqrt{s} = 1.96$ TeV*, Phys. Rev. Lett. **91** (2003) 241804, arXiv:hep-ex/0307080.
- [10] CDF collaboration, T. A. Aaltonen *et al.*, *Measurement of the D^+ meson production cross section at low transverse momentum in $p\bar{p}$ collisions at $\sqrt{s} = 1.96$ TeV*, Phys. Rev. **D95** (2017) 092006, arXiv:1610.08989.
- [11] UA1 collaboration, C. Albajar *et al.*, *Measurement of the bottom quark production cross-section in proton-antiproton collisions at $\sqrt{s} = 0.63$ TeV*, Phys. Lett. **B213** (1988) 405.
- [12] D0 collaboration, S. Abachi *et al.*, *Inclusive μ and b quark production cross-sections in $p\bar{p}$ collisions at $\sqrt{s} = 1.8$ TeV*, Phys. Rev. Lett. **74** (1995) 3548.
- [13] CDF collaboration, F. Abe *et al.*, *Measurement of the B meson differential cross-section, $d\sigma/dp_T$, in $p\bar{p}$ collisions at $\sqrt{s} = 1.8$ TeV*, Phys. Rev. Lett. **75** (1995) 1451, arXiv:hep-ex/9503013.

- [14] CDF collaboration, A. Abulencia *et al.*, *Measurement of the B^+ production cross-section in $p\bar{p}$ collisions at $\sqrt{s} = 1960$ GeV*, Phys. Rev. **D75** (2007) 012010, [arXiv:hep-ex/0612015](#).
- [15] LHCb collaboration, R. Aaij *et al.*, *Measurement of $\sigma(pp \rightarrow b\bar{b}X)$ at $\sqrt{s} = 7$ TeV in the forward region*, Phys. Lett. **B694** (2010) 209, [arXiv:1009.2731](#).
- [16] CMS collaboration, V. Khachatryan *et al.*, *Inclusive b-hadron production cross section with muons in pp collisions at $\sqrt{s} = 7$ TeV*, JHEP **03** (2011) 090, [arXiv:1101.3512](#).
- [17] LHCb collaboration, R. Aaij *et al.*, *Measurement of J/ψ production in pp collisions at $\sqrt{s} = 7$ TeV*, Eur. Phys. J. **C71** (2011) 1645, [arXiv:1103.0423](#).
- [18] LHCb collaboration, R. Aaij *et al.*, *Production of J/ψ and Υ mesons in pp collisions at $\sqrt{s} = 8$ TeV*, JHEP **06** (2013) 064, [arXiv:1304.6977](#).
- [19] LHCb collaboration, R. Aaij *et al.*, *Measurement of forward J/ψ production cross-sections in pp collisions at $\sqrt{s} = 13$ TeV*, JHEP **10** (2015) 172, [arXiv:1509.00771](#).
- [20] LHCb collaboration, R. Aaij *et al.*, *Measurement of the B^\pm production cross-section in pp collisions at $\sqrt{s} = 7$ TeV*, JHEP **04** (2012) 093, [arXiv:1202.4812](#).
- [21] LHCb collaboration, R. Aaij *et al.*, *Measurement of B meson production cross-sections in proton-proton collisions at $\sqrt{s} = 7$ TeV*, JHEP **08** (2013) 117, [arXiv:1306.3663](#).
- [22] CMS collaboration, V. Khachatryan *et al.*, *Measurement of the B^+ production cross section in pp collisions at $\sqrt{s} = 7$ TeV*, Phys. Rev. Lett. **106** (2011) 112001, [arXiv:1101.0131](#).
- [23] CMS collaboration, S. Chatrchyan *et al.*, *Measurement of the B^0 production cross section in pp collisions at $\sqrt{s} = 7$ TeV*, Phys. Rev. Lett. **106** (2011) 252001, [arXiv:1104.2892](#).
- [24] LHCb collaboration, R. Aaij *et al.*, *Study of the productions of Λ_b^0 and \bar{B}^0 hadrons in pp collisions and first measurement of the $\Lambda_b^0 \rightarrow J/\psi p K^-$ branching fraction*, Chin. Phys. C **40** (2016) 011001, [arXiv:1509.00292](#).
- [25] CMS collaboration, S. Chatrchyan *et al.*, *Measurement of the Λ_b^0 cross section and the $\bar{\Lambda}_b^0$ to Λ_b^0 ratio with $J/\psi \Lambda$ decays in pp collisions at $\sqrt{s} = 7$ TeV*, Phys. Lett. **B714** (2012) 136, [arXiv:1205.0594](#).
- [26] LHCb collaboration, R. Aaij *et al.*, *Measurements of B_c^+ production and mass with the $B_c^+ \rightarrow J/\psi \pi^+$ decay*, Phys. Rev. Lett. **109** (2012) 232001, [arXiv:1209.5634](#).
- [27] LHCb collaboration, R. Aaij *et al.*, *Measurement of B_c^+ production at $\sqrt{s} = 8$ TeV*, Phys. Rev. Lett. **114** (2015) 132001, [arXiv:1411.2943](#).
- [28] B. A. Kniehl, G. Kramer, I. Schienbein, and H. Spiesberger, *Inclusive charmed-meson production at the CERN LHC*, Eur. Phys. J. **C72** (2012) 2082, [arXiv:1202.0439](#).
- [29] B. A. Kniehl, G. Kramer, I. Schienbein, and H. Spiesberger, *Inclusive $D^{*\pm}$ production in $p\bar{p}$ collisions with massive charm quarks*, Phys. Rev. **D71** (2005) 014018, [arXiv:hep-ph/0410289](#).

- [30] B. A. Kniehl, G. Kramer, I. Schienbein, and H. Spiesberger, *Reconciling open charm production at the Fermilab Tevatron with QCD*, Phys. Rev. Lett. **96** (2006) 012001, arXiv:hep-ph/0508129.
- [31] T. Kneesch, B. A. Kniehl, G. Kramer, and I. Schienbein, *Charmed-meson fragmentation functions with finite-mass corrections*, Nucl. Phys. **B799** (2008) 34, arXiv:0712.0481.
- [32] B. A. Kniehl, G. Kramer, I. Schienbein, and H. Spiesberger, *Open charm hadroproduction and the charm content of the proton*, Phys. Rev. **D79** (2009) 094009, arXiv:0901.4130.
- [33] R. Gauld, J. Rojo, L. Rottoli, and J. Talbert, *Charm production in the forward region: constraints on the small- x gluon and backgrounds for neutrino astronomy*, JHEP **11** (2015) 009, arXiv:1506.08025.
- [34] M. Cacciari, M. Greco, and P. Nason, *The p_T spectrum in heavy flavor hadroproduction*, JHEP **05** (1998) 007, arXiv:hep-ph/9803400.
- [35] M. Cacciari, S. Frixione, and P. Nason, *The p_T spectrum in heavy flavor photoproduction*, JHEP **03** (2001) 006, arXiv:hep-ph/0102134.
- [36] M. Cacciari and P. Nason, *Charm cross-sections for the Tevatron Run II*, JHEP **09** (2003) 006, arXiv:hep-ph/0306212.
- [37] M. Cacciari, P. Nason, and C. Oleari, *A study of heavy flavored meson fragmentation functions in e^+e^- annihilation*, JHEP **04** (2006) 006, arXiv:hep-ph/0510032.
- [38] M. Cacciari *et al.*, *Theoretical predictions for charm and bottom production at the LHC*, JHEP **10** (2012) 137, arXiv:1205.6344.
- [39] M. Cacciari, M. L. Mangano, and P. Nason, *Gluon PDF constraints from the ratio of forward heavy-quark production at the LHC at $\sqrt{s} = 7$ and 13 TeV*, Eur. Phys. J. **C75** (2015) 610, arXiv:1507.06197.
- [40] C.-H. Chang and Y.-Q. Chen, *The hadronic production of the B_c^+ meson at Tevatron, CERN LHC and SSC*, Phys. Rev. **D48** (1993) 4086.
- [41] C.-H. Chang, Y.-Q. Chen, G.-P. Han, and H.-T. Jiang, *On hadronic production of the B_c^+ meson*, Phys. Lett. **B364** (1995) 78, arXiv:hep-ph/9408242.
- [42] A. V. Berezhnoy, A. K. Likhoded, and M. V. Shevlyagin, *Hadronic production of B_c^+ mesons*, Phys. Atom. Nucl. **58** (1995) 672, arXiv:hep-ph/9408284, [Yad. Fiz. **58** (1995) 730].
- [43] K. Kołodziej, A. Leike, and R. Rückl, *Production of B_c^+ mesons in hadronic collisions*, Phys. Lett. **B355** (1995) 337, arXiv:hep-ph/9505298.
- [44] CDF collaboration, B. Reisert *et al.*, *Charm production studies at CDF*, Nucl. Phys. Proc. Suppl. **170** (2007) 243.

- [45] CDF and D0 collaborations, B. Reiser, *Charm and beauty production at the Tevatron*, in *Proceedings, 15th International Workshop on deep-inelastic scattering and related subjects (DIS 2007)*, p. 829, 2007. doi: 10.3204/proc07-01/150.
- [46] LHCb collaboration, R. Aaij *et al.*, *Observation of double charm production involving open charm in pp collisions at $\sqrt{s} = 7$ TeV*, JHEP **06** (2012) 141, Addendum *ibid.* **03** (2014) 108, arXiv:1205.0975.
- [47] UA1 collaboration, C. Albajar *et al.*, *Measurement of $b\bar{b}$ correlations at the CERN $p\bar{p}$ collider*, Z. Phys. **C61** (1994) 41.
- [48] D0 collaboration, B. Abbott *et al.*, *The $b\bar{b}$ production cross section and angular correlations in $p\bar{p}$ collisions at $\sqrt{s} = 1.8$ TeV*, Phys. Lett. **B487** (2000) 264, arXiv:hep-ex/9905024.
- [49] CDF collaboration, F. Abe *et al.*, *Measurement of $b\bar{b}$ production correlations, $B^0\bar{B}^0$ mixing, and a limit on ϵ_B in $p\bar{p}$ collisions at $\sqrt{s} = 1.8$ TeV*, Phys. Rev. **D55** (1997) 2546.
- [50] CDF collaboration, F. Abe *et al.*, *Measurement of $b\bar{b}$ rapidity correlations in $p\bar{p}$ collisions at $\sqrt{s} = 1.8$ TeV*, Phys. Rev. **D61** (2000) 032001.
- [51] CDF collaboration, D. Acosta *et al.*, *Measurements of $b\bar{b}$ azimuthal production correlations in $p\bar{p}$ collisions at $\sqrt{s} = 1.8$ TeV*, Phys. Rev. **D71** (2005) 092001, arXiv:hep-ex/0412006.
- [52] CDF collaboration, T. Aaltonen *et al.*, *Measurement of correlated $b\bar{b}$ production in $p\bar{p}$ collisions at $\sqrt{s} = 1960$ GeV*, Phys. Rev. **D77** (2008) 072004, arXiv:0710.1895.
- [53] CMS collaboration, V. Khachatryan *et al.*, *Measurement of $B\bar{B}$ angular correlations based on secondary vertex reconstruction at $\sqrt{s} = 7$ TeV*, JHEP **03** (2011) 136, arXiv:1102.3194.
- [54] S. Frixione and B. R. Webber, *Matching NLO QCD computations and parton shower simulations*, JHEP **06** (2002) 029, arXiv:hep-ph/0204244; S. Frixione, P. Nason, and B. R. Webber, *Matching NLO QCD and parton showers in heavy flavor production*, JHEP **08** (2003) 007, arXiv:hep-ph/0305252; S. Frixione and B. R. Webber, *The MC@NLO 3.4 event generator*, arXiv:0812.0770.
- [55] H. Jung and G. P. Salam, *Hadronic final state predictions from CCFM: The hadron level Monte Carlo generator CASCADE*, Eur. Phys. J. **C19** (2001) 351, arXiv:hep-ph/0012143; S. Catani, M. Ciafaloni, and F. Hautmann, *High-energy factorization in QCD and minimal subtraction scheme*, Phys. Lett. **B307** (1993) 147.
- [56] T. Sjöstrand, S. Mrenna, and P. Skands, *A brief introduction to PYTHIA 8.1*, Comput. Phys. Commun. **178** (2008) 852, arXiv:0710.3820.
- [57] F. Maltoni and T. Stelzer, *MAD EVENT: Automatic event generation with MADGRAPH*, JHEP **02** (2003) 027, arXiv:hep-ph/0208156; J. Alwall *et al.*, *MADGRAPH/MAD EVENT V4: The new web generation*, JHEP **09** (2007) 028, arXiv:0706.2334.

- [58] ATLAS collaboration, M. Aaboud *et al.*, *Measurement of b-hadron pair production with the ATLAS detector in proton-proton collisions at $\sqrt{s} = 8$ TeV*, arXiv:1705.03374.
- [59] J. Alwall *et al.*, *The automated computation of tree-level and next-to-leading order differential cross sections, and their matching to parton shower simulations*, JHEP **07** (2014) 079, arXiv:1405.0301.
- [60] M. Bahr *et al.*, HERWIG++ *Physics and Manual*, Eur. Phys. J. **C58** (2008) 639, arXiv:0803.0883.
- [61] T. Sjöstrand, S. Mrenna, and P. Skands, *PYTHIA 6.4 physics and manual*, JHEP **05** (2006) 026, arXiv:hep-ph/0603175.
- [62] P. Nason, *A new method for combining NLO QCD with shower Monte Carlo algorithms*, JHEP **11** (2004) 040, arXiv:hep-ph/0409146.
- [63] S. Frixione, P. Nason, and C. Oleari, *Matching NLO QCD computations with parton shower simulations: the POWHEG method*, JHEP **11** (2007) 070, arXiv:0709.2092.
- [64] S. Frixione, P. Nason, and G. Ridolfi, *A positive-weight next-to-leading-order Monte Carlo for heavy flavour hadroproduction*, JHEP **09** (2007) 126, arXiv:0707.3088.
- [65] S. Alioli, P. Nason, C. Oleari, and E. Re, *A general framework for implementing NLO calculations in shower Monte Carlo programs: the POWHEG BOX*, JHEP **06** (2010) 043, arXiv:1002.2581.
- [66] LHCb collaboration, A. A. Alves Jr. *et al.*, *The LHCb detector at the LHC*, JINST **3** (2008) S08005.
- [67] LHCb collaboration, R. Aaij *et al.*, *LHCb detector performance*, Int. J. Mod. Phys. **A30** (2015) 1530022, arXiv:1412.6352.
- [68] R. Aaij *et al.*, *Performance of the LHCb Vertex Locator*, JINST **9** (2014) P09007, arXiv:1405.7808.
- [69] A. A. Alves Jr. *et al.*, *Performance of the LHCb muon system*, JINST **8** (2013) P02022, arXiv:1211.1346.
- [70] R. Aaij *et al.*, *The LHCb trigger and its performance in 2011*, JINST **8** (2013) P04022, arXiv:1211.3055.
- [71] I. Belyaev *et al.*, *Handling of the generation of primary events in GAUSS, the LHCb simulation framework*, J. Phys. Conf. Ser. **331** (2011) 032047.
- [72] D. J. Lange, *The EVTGEN particle decay simulation package*, Nucl. Instrum. Meth. **A462** (2001) 152.
- [73] P. Golonka and Z. Was, *PHOTOS Monte Carlo: A precision tool for QED corrections in Z and W decays*, Eur. Phys. J. **C45** (2006) 97, arXiv:hep-ph/0506026.

- [74] Geant4 collaboration, J. Allison *et al.*, *GEANT4 developments and applications*, IEEE Trans. Nucl. Sci. **53** (2006) 270; Geant4 collaboration, S. Agostinelli *et al.*, *GEANT4: A simulation toolkit*, Nucl. Instrum. Meth. **A506** (2003) 250.
- [75] M. Clemencic *et al.*, *The LHCb simulation application, GAUSS: Design, evolution and experience*, J. Phys. Conf. Ser. **331** (2011) 032023.
- [76] F. Archilli *et al.*, *Performance of the muon identification at LHCb*, JINST **8** (2013) P10020, [arXiv:1306.0249](#).
- [77] T. Skwarnicki, *A study of the radiative cascade transitions between the Υ' and Υ resonances*, PhD thesis, Institute of Nuclear Physics, Krakow, 1986, DESY-F31-86-02.
- [78] LHCb collaboration, R. Aaij *et al.*, *Observation of J/ψ -pair production in pp collisions at $\sqrt{s} = 7$ TeV*, Phys. Lett. **B707** (2012) 52, [arXiv:1109.0963](#).
- [79] LHCb collaboration, R. Aaij *et al.*, *Measurement of the J/ψ pair production cross-section in pp collisions at $\sqrt{s} = 13$ TeV*, JHEP **06** (2017) 047, [arXiv:1612.07451](#).
- [80] LHCb collaboration, R. Aaij *et al.*, *Production of associated Υ and open charm hadrons in pp collisions at $\sqrt{s} = 7$ and 8 TeV via double parton scattering*, JHEP **07** (2016) 052, [arXiv:1510.05949](#).
- [81] LHCb collaboration, R. Aaij *et al.*, *Observation of associated production of a Z boson with a D meson in the forward region*, JHEP **04** (2014) 091, [arXiv:1401.3245](#).
- [82] M. Pivk and F. R. Le Diberder, *sPlot: A statistical tool to unfold data distributions*, Nucl. Instrum. Meth. **A555** (2005) 356, [arXiv:physics/0402083](#).
- [83] D. Martínez Santos and F. Dupertuis, *Mass distributions marginalized over per-event errors*, Nucl. Instrum. Meth. **A764** (2014) 150, [arXiv:1312.5000](#).
- [84] LHCb collaboration, R. Aaij *et al.*, *Measurement of the track reconstruction efficiency at LHCb*, JINST **10** (2015) P02007, [arXiv:1408.1251](#).
- [85] H.-L. Lai *et al.*, *Parton distributions for event generators*, JHEP **04** (2010) 035, [arXiv:0910.4183](#).
- [86] J. Pumplin *et al.*, *New generation of parton distributions with uncertainties from global QCD analysis*, JHEP **07** (2002) 012, [arXiv:hep-ph/0201195](#).
- [87] P. M. Nadolsky *et al.*, *Implications of CTEQ global analysis for collider observables*, Phys. Rev. **D78** (2008) 013004, [arXiv:0802.0007](#).
- [88] P. Nason, S. Dawson, and R. K. Ellis, *The total cross-section for the production of heavy quarks in hadronic collisions*, Nucl. Phys. **B303** (1988) 607.

LHCb collaboration

R. Aaij⁴⁰, B. Adeva³⁹, M. Adinolfi⁴⁸, Z. Ajaltouni⁵, S. Akar⁵⁹, J. Albrecht¹⁰, F. Alessio⁴⁰, M. Alexander⁵³, A. Alfonso Alberio³⁸, S. Ali⁴³, G. Alkhazov³¹, P. Alvarez Cartelle⁵⁵, A.A. Alves Jr⁵⁹, S. Amato², S. Amerio²³, Y. Amhis⁷, L. An³, L. Anderlini¹⁸, G. Andreassi⁴¹, M. Andreotti^{17,g}, J.E. Andrews⁶⁰, R.B. Appleby⁵⁶, F. Archilli⁴³, P. d'Argent¹², J. Arnau Romeu⁶, A. Artamonov³⁷, M. Artuso⁶¹, E. Aslanides⁶, G. Auriemma²⁶, M. Baalouch⁵, I. Babuschkin⁵⁶, S. Bachmann¹², J.J. Back⁵⁰, A. Badalov^{38,m}, C. Baesso⁶², S. Baker⁵⁵, V. Balagura^{7,b}, W. Baldini¹⁷, A. Baranov³⁵, R.J. Barlow⁵⁶, C. Barschel⁴⁰, S. Barsuk⁷, W. Barter⁵⁶, F. Baryshnikov³², V. Batozskaya²⁹, V. Battista⁴¹, A. Bay⁴¹, L. Beaucourt⁴, J. Beddow⁵³, F. Bedeschi²⁴, I. Bediaga¹, A. Beiter⁶¹, L.J. Bel⁴³, N. Bely⁶³, V. Bellec⁴¹, N. Belloli^{21,i}, K. Belous³⁷, I. Belyaev³², E. Ben-Haim⁸, G. Bencivenni¹⁹, S. Benson⁴³, S. Beranek⁹, A. Berezhnoy³³, R. Bernet⁴², D. Berninghoff¹², E. Bertholet⁸, A. Bertolin²³, C. Betancourt⁴², F. Betti¹⁵, M.-O. Bettler⁴⁰, M. van Beuzekom⁴³, I.a. Bezshyiko⁴², S. Bifani⁴⁷, P. Billoir⁸, A. Birnkraut¹⁰, A. Bitadze⁵⁶, A. Bizzeti^{18,u}, M. Bjørn⁵⁷, T. Blake⁵⁰, F. Blanc⁴¹, J. Blouw^{11,†}, S. Blusk⁶¹, V. Bocci²⁶, T. Boettcher⁵⁸, A. Bondar^{36,w}, N. Bondar³¹, W. Bonivento¹⁶, I. Bordyuzhin³², A. Borgheresi^{21,i}, S. Borghi⁵⁶, M. Borisyak³⁵, M. Borsato³⁹, F. Bossu⁷, M. Boubdir⁹, T.J.V. Bowcock⁵⁴, E. Bowen⁴², C. Bozzi^{17,40}, S. Braun¹², T. Britton⁶¹, J. Brodzicka²⁷, D. Brundu¹⁶, E. Buchanan⁴⁸, C. Burr⁵⁶, A. Bursche^{16,f}, J. Buytaert⁴⁰, W. Byczynski⁴⁰, S. Cadeddu¹⁶, H. Cai⁶⁴, R. Calabrese^{17,g}, R. Calladine⁴⁷, M. Calvi^{21,i}, M. Calvo Gomez^{38,m}, A. Camboni^{38,m}, P. Campana¹⁹, D.H. Campora Perez⁴⁰, L. Capriotti⁵⁶, A. Carbone^{15,e}, G. Carboni^{25,j}, R. Cardinale^{20,h}, A. Cardini¹⁶, P. Carniti^{21,i}, L. Carson⁵², K. Carvalho Akiba², G. Casse⁵⁴, L. Cassina²¹, L. Castillo Garcia⁴¹, M. Cattaneo⁴⁰, G. Cavallero^{20,40,h}, R. Cenci^{24,t}, D. Chamont⁷, M.G. Chapman⁴⁸, M. Charles⁸, Ph. Charpentier⁴⁰, G. Chatzikonstantinidis⁴⁷, M. Chefdeville⁴, S. Chen⁵⁶, S.F. Cheung⁵⁷, S.-G. Chitic⁴⁰, V. Chobanova³⁹, M. Chrzaszcz^{42,27}, A. Chubykin³¹, P. Ciambone¹⁹, X. Cid Vidal³⁹, G. Ciezarek⁴³, P.E.L. Clarke⁵², M. Clemencic⁴⁰, H.V. Cliff⁴⁹, J. Closier⁴⁰, J. Cogan⁶, E. Cogneras⁵, V. Cogoni^{16,f}, L. Cojocariu³⁰, P. Collins⁴⁰, T. Colombo⁴⁰, A. Comerma-Montells¹², A. Contu⁴⁰, A. Cook⁴⁸, G. Coombs⁴⁰, S. Coquereau³⁸, G. Corti⁴⁰, M. Corvo^{17,g}, C.M. Costa Sobral⁵⁰, B. Couturier⁴⁰, G.A. Cowan⁵², D.C. Craik⁵⁸, A. Crocombe⁵⁰, M. Cruz Torres¹, R. Currie⁵², C. D'Ambrosio⁴⁰, F. Da Cunha Marinho², E. Dall'Occo⁴³, J. Dalseno⁴⁸, A. Davis³, O. De Aguiar Francisco⁵⁴, S. De Capua⁵⁶, M. De Cian¹², J.M. De Miranda¹, L. De Paula², M. De Serio^{14,d}, P. De Simone¹⁹, C.T. Dean⁵³, D. Decamp⁴, L. Del Buono⁸, H.-P. Dembinski¹¹, M. Demmer¹⁰, A. Dendek²⁸, D. Derkach³⁵, O. Deschamps⁵, F. Dettori⁵⁴, B. Dey⁶⁵, A. Di Canto⁴⁰, P. Di Nezza¹⁹, H. Dijkstra⁴⁰, F. Dordei⁴⁰, M. Dorigo⁴⁰, A. Dosil Suárez³⁹, L. Douglas⁵³, A. Dovbnya⁴⁵, K. Dreimanis⁵⁴, L. Dufour⁴³, G. Dujany⁸, P. Durante⁴⁰, R. Dzhelyadin³⁷, M. Dziewiecki¹², A. Dziurda⁴⁰, A. Dzyuba³¹, S. Easo⁵¹, M. Ebert⁵², U. Egede⁵⁵, V. Egorychev³², S. Eidelman^{36,w}, S. Eisenhardt⁵², U. Eitschberger¹⁰, R. Ekelhof¹⁰, L. Eklund⁵³, S. Ely⁶¹, S. Esen¹², H.M. Evans⁴⁹, T. Evans⁵⁷, A. Falabella¹⁵, N. Farley⁴⁷, S. Farry⁵⁴, R. Fay⁵⁴, D. Fazzini^{21,i}, L. Federici²⁵, D. Ferguson⁵², G. Fernandez³⁸, P. Fernandez Declara⁴⁰, A. Fernandez Prieto³⁹, F. Ferrari¹⁵, F. Ferreira Rodrigues², M. Ferro-Luzzi⁴⁰, S. Filippov³⁴, R.A. Fini¹⁴, M. Fiore^{17,g}, M. Fiorini^{17,g}, M. Firlej²⁸, C. Fitzpatrick⁴¹, T. Fiutowski²⁸, F. Fleuret^{7,b}, K. Fohl⁴⁰, M. Fontana^{16,40}, F. Fontanelli^{20,h}, D.C. Forshaw⁶¹, R. Forty⁴⁰, V. Franco Lima⁵⁴, M. Frank⁴⁰, C. Frei⁴⁰, J. Fu^{22,q}, W. Funk⁴⁰, E. Furfaro^{25,j}, C. Färber⁴⁰, E. Gabriel⁵², A. Gallas Torreira³⁹, D. Galli^{15,e}, S. Gallorini²³, S. Gambetta⁵², M. Gandelman², P. Gandini⁵⁷, Y. Gao³, L.M. Garcia Martin⁷⁰, J. García Pardiñas³⁹, J. Garra Tico⁴⁹, L. Garrido³⁸, P.J. Garsed⁴⁹, D. Gascon³⁸, C. Gaspar⁴⁰, L. Gavardi¹⁰, G. Gazzoni⁵, D. Gerick¹², E. Gersabeck¹², M. Gersabeck⁵⁶, T. Gershon⁵⁰, Ph. Ghez⁴, S. Gianì⁴¹, V. Gibson⁴⁹, O.G. Girard⁴¹, L. Giubega³⁰, K. Gizdov⁵², V.V. Gligorov⁸, D. Golubkov³², A. Golutvin^{55,40}, A. Gomes^{1,a},

I.V. Gorelov³³, C. Gotti^{21,i}, E. Govorkova⁴³, J.P. Grabowski¹², R. Graciani Diaz³⁸,
 L.A. Granado Cardoso⁴⁰, E. Graugés³⁸, E. Graverini⁴², G. Graziani¹⁸, A. Grecu³⁰, R. Greim⁹,
 P. Griffith¹⁶, L. Grillo^{21,40,i}, L. Gruber⁴⁰, B.R. Gruberg Cazon⁵⁷, O. Grünberg⁶⁷, E. Gushchin³⁴,
 Yu. Guz³⁷, T. Gys⁴⁰, C. Göbel⁶², T. Hadavizadeh⁵⁷, C. Hadjivasiliou⁵, G. Haefeli⁴¹, C. Haen⁴⁰,
 S.C. Haines⁴⁹, B. Hamilton⁶⁰, X. Han¹², T.H. Hancock⁵⁷, S. Hansmann-Menzemer¹²,
 N. Harnew⁵⁷, S.T. Harnew⁴⁸, J. Harrison⁵⁶, C. Hasse⁴⁰, M. Hatch⁴⁰, J. He⁶³, M. Hecker⁵⁵,
 K. Heinicke¹⁰, A. Heister⁹, K. Hennessy⁵⁴, P. Henrard⁵, L. Henry⁷⁰, E. van Herwijnen⁴⁰,
 M. Heß⁶⁷, A. Hicheur², D. Hill⁵⁷, C. Hombach⁵⁶, P.H. Hopchev⁴¹, Z.C. Huard⁵⁹,
 W. Hulsbergen⁴³, T. Humair⁵⁵, M. Hushchyn³⁵, D. Hutchcroft⁵⁴, P. Ibis¹⁰, M. Idzik²⁸,
 P. Ilten⁵⁸, R. Jacobsson⁴⁰, J. Jalocho⁵⁷, E. Jans⁴³, A. Jawahery⁶⁰, F. Jiang³, M. John⁵⁷,
 D. Johnson⁴⁰, C.R. Jones⁴⁹, C. Joram⁴⁰, B. Jost⁴⁰, N. Jurik⁵⁷, S. Kandybei⁴⁵, M. Karacson⁴⁰,
 J.M. Kariuki⁴⁸, S. Karodia⁵³, N. Kazeev³⁵, M. Kecke¹², M. Kelsey⁶¹, M. Kenzie⁴⁹, T. Ketel⁴⁴,
 E. Khairullin³⁵, B. Khanji¹², C. Khurewathanakul⁴¹, T. Kirn⁹, S. Klaver⁵⁶, K. Klimaszewski²⁹,
 T. Klimkovich¹¹, S. Koliiev⁴⁶, M. Kolpin¹², I. Komarov⁴¹, R. Kopečna¹², P. Koppenburg⁴³,
 A. Kosmyntseva³², S. Kotriakhova³¹, M. Kozeiha⁵, L. Kravchuk³⁴, M. Kreps⁵⁰, P. Krokovny^{36,w},
 F. Kruse¹⁰, W. Krzemien²⁹, W. Kucewicz^{27,l}, M. Kucharczyk²⁷, V. Kudryavtsev^{36,w},
 A.K. Kuonen⁴¹, K. Kurek²⁹, T. Kvaratskheliya^{32,40}, D. Lacarrere⁴⁰, G. Lafferty⁵⁶, A. Lai¹⁶,
 G. Lanfranchi¹⁹, C. Langenbruch⁹, T. Latham⁵⁰, C. Lazzeroni⁴⁷, R. Le Gac⁶, A. Leflat^{33,40},
 J. Lefrançois⁷, R. Lefèvre⁵, F. Lemaitre⁴⁰, E. Lemos Cid³⁹, O. Leroy⁶, T. Lesiak²⁷,
 B. Leverington¹², P.-R. Li⁶³, T. Li³, Y. Li⁷, Z. Li⁶¹, T. Likhomanenko⁶⁸, R. Lindner⁴⁰,
 F. Lionetto⁴², V. Lisovskyi⁷, X. Liu³, D. Loh⁵⁰, A. Loi¹⁶, I. Longstaff⁵³, J.H. Lopes²,
 D. Lucchesi^{23,o}, A. Luchinsky³⁷, M. Lucio Martinez³⁹, H. Luo⁵², A. Lupato²³, E. Luppi^{17,g},
 O. Lupton⁴⁰, A. Lusiani²⁴, X. Lyu⁶³, F. Machefert⁷, F. Maciuc³⁰, V. Macko⁴¹, P. Mackowiak¹⁰,
 S. Maddrell-Mander⁴⁸, O. Maev^{31,40}, K. Maguire⁵⁶, D. Maisuzenko³¹, M.W. Majewski²⁸,
 S. Malde⁵⁷, A. Malinin⁶⁸, T. Maltsev^{36,w}, G. Manca^{16,f}, G. Mancinelli⁶, P. Manning⁶¹,
 D. Marangotto^{22,q}, J. Maratas^{5,v}, J.F. Marchand⁴, U. Marconi¹⁵, C. Marin Benito³⁸,
 M. Marinangeli⁴¹, P. Marino⁴¹, J. Marks¹², G. Martellotti²⁶, M. Martin⁶, M. Martinelli⁴¹,
 D. Martinez Santos³⁹, F. Martinez Vidal⁷⁰, D. Martins Tostes², L.M. Massacrier⁷,
 A. Massafferri¹, R. Matev⁴⁰, A. Mathad⁵⁰, Z. Mathe⁴⁰, C. Matteuzzi²¹, A. Mauri⁴²,
 E. Maurice^{7,b}, B. Maurin⁴¹, A. Mazurov⁴⁷, M. McCann^{55,40}, A. McNab⁵⁶, R. McNulty¹³,
 J.V. Mead⁵⁴, B. Meadows⁵⁹, C. Meaux⁶, F. Meier¹⁰, N. Meinert⁶⁷, D. Melnychuk²⁹, M. Merk⁴³,
 A. Merli^{22,40,q}, E. Michielin²³, D.A. Milanese⁶⁶, E. Millard⁵⁰, M.-N. Minard⁴, L. Minzoni¹⁷,
 D.S. Mitzel¹², A. Mogini⁸, J. Molina Rodriguez¹, T. Mombächer¹⁰, I.A. Monroy⁶⁶, S. Monteil⁵,
 M. Morandin²³, M.J. Morello^{24,t}, O. Morgunova⁶⁸, J. Moron²⁸, A.B. Morris⁵², R. Mountain⁶¹,
 F. Muheim⁵², M. Mulder⁴³, D. Müller⁵⁶, J. Müller¹⁰, K. Müller⁴², V. Müller¹⁰, P. Naik⁴⁸,
 T. Nakada⁴¹, R. Nandakumar⁵¹, A. Nandi⁵⁷, I. Nasteva², M. Needham⁵², N. Neri^{22,40},
 S. Neubert¹², N. Neufeld⁴⁰, M. Neuner¹², T.D. Nguyen⁴¹, C. Nguyen-Mau^{41,n}, S. Nieswand⁹,
 R. Niet¹⁰, N. Nikitin³³, T. Nikodem¹², A. Nogay⁶⁸, D.P. O’Hanlon⁵⁰, A. Oblakowska-Mucha²⁸,
 V. Obraztsov³⁷, S. Ogilvy¹⁹, R. Oldeman^{16,f}, C.J.G. Onderwater⁷¹, A. Ossowska²⁷,
 J.M. Otalora Goicochea², P. Owen⁴², A. Oyanguren⁷⁰, P.R. Pais⁴¹, A. Palano^{14,d},
 M. Palutan^{19,40}, A. Papanestis⁵¹, M. Pappagallo^{14,d}, L.L. Pappalardo^{17,g}, W. Parker⁶⁰,
 C. Parkes⁵⁶, G. Passaleva¹⁸, A. Pastore^{14,d}, M. Patel⁵⁵, C. Patrignani^{15,e}, A. Pearce⁴⁰,
 A. Pellegrino⁴³, G. Penso²⁶, M. Pepe Altarelli⁴⁰, S. Perazzini⁴⁰, P. Perret⁵, L. Pescatore⁴¹,
 K. Petridis⁴⁸, A. Petrolini^{20,h}, A. Petrov⁶⁸, M. Petruzzo^{22,q}, E. Picatoste Olloqui³⁸,
 B. Pietrzyk⁴, M. Pikies²⁷, D. Pinci²⁶, F. Pisani⁴⁰, A. Pistone^{20,h}, A. Piucci¹², V. Placinta³⁰,
 S. Playfer⁵², M. Plo Casasus³⁹, F. Polci⁸, M. Poli Lener¹⁹, A. Poluektov^{50,36}, I. Polyakov⁶¹,
 E. Polycarpo², G.J. Pomery⁴⁸, S. Ponce⁴⁰, A. Popov³⁷, D. Popov^{11,40}, S. Poslavskii³⁷,
 C. Potterat², E. Price⁴⁸, J. Prisciandaro³⁹, C. Prouve⁴⁸, V. Pugatch⁴⁶, A. Puig Navarro⁴²,
 H. Pullen⁵⁷, G. Punzi^{24,p}, W. Qian⁵⁰, R. Quagliani^{7,48}, B. Quintana⁵, B. Rachwal²⁸,
 J.H. Rademacker⁴⁸, M. Rama²⁴, M. Ramos Pernas³⁹, M.S. Rangel², I. Raniuk^{45,†},

F. Ratnikov³⁵, G. Raven⁴⁴, M. Ravonel Salzgeber⁴⁰, M. Reboud⁴, F. Redi⁵⁵, S. Reichert¹⁰, A.C. dos Reis¹, C. Remon Alepuz⁷⁰, V. Renaudin⁷, S. Ricciardi⁵¹, S. Richards⁴⁸, M. Rihl⁴⁰, K. Rinnert⁵⁴, V. Rives Molina³⁸, P. Robbe⁷, A. Robert⁸, A.B. Rodrigues¹, E. Rodrigues⁵⁹, J.A. Rodriguez Lopez⁶⁶, P. Rodriguez Perez^{56,†}, A. Rogozhnikov³⁵, S. Roiser⁴⁰, A. Rollings⁵⁷, V. Romanovskiy³⁷, A. Romero Vidal³⁹, J.W. Ronayne¹³, M. Rotondo¹⁹, M.S. Rudolph⁶¹, T. Ruf⁴⁰, P. Ruiz Valls⁷⁰, J. Ruiz Vidal⁷⁰, J.J. Saborido Silva³⁹, E. Sadykhov³², N. Sagidova³¹, B. Saitta^{16,f}, V. Salustino Guimaraes¹, C. Sanchez Mayordomo⁷⁰, B. Sanmartin Sedes³⁹, R. Santacesaria²⁶, C. Santamarina Rios³⁹, M. Santimaria¹⁹, E. Santovetti^{25,j}, G. Sarpis⁵⁶, A. Sarti²⁶, C. Satriano^{26,s}, A. Satta²⁵, D.M. Saunders⁴⁸, D. Savrina^{32,33}, S. Schael⁹, M. Schellenberg¹⁰, M. Schiller⁵³, H. Schindler⁴⁰, M. Schlupp¹⁰, M. Schmelling¹¹, T. Schmelzer¹⁰, B. Schmidt⁴⁰, O. Schneider⁴¹, A. Schopper⁴⁰, H.F. Schreiner⁵⁹, K. Schubert¹⁰, M. Schubiger⁴¹, M.-H. Schune⁷, R. Schwemmer⁴⁰, B. Sciascia¹⁹, A. Sciubba^{26,k}, A. Semennikov³², E.S. Sepulveda⁸, A. Sergi⁴⁷, N. Serra⁴², J. Serrano⁶, L. Sestini²³, P. Seyfert⁴⁰, M. Shapkin³⁷, I. Shapoval⁴⁵, Y. Shcheglov³¹, T. Shears⁵⁴, L. Shekhtman^{36,w}, V. Shevchenko⁶⁸, B.G. Siddi^{17,40}, R. Silva Coutinho⁴², L. Silva de Oliveira², G. Simi^{23,o}, S. Simone^{14,d}, M. Sirendi⁴⁹, N. Skidmore⁴⁸, T. Skwarnicki⁶¹, E. Smith⁵⁵, I.T. Smith⁵², J. Smith⁴⁹, M. Smith⁵⁵, I. Soares Lavra¹, M.D. Sokoloff⁵⁹, F.J.P. Soler⁵³, B. Souza De Paula², B. Spaan¹⁰, P. Spradlin⁵³, S. Sridharan⁴⁰, F. Stagni⁴⁰, M. Stahl¹², S. Stahl⁴⁰, P. Stefko⁴¹, S. Stefkova⁵⁵, O. Steinkamp⁴², S. Stemmler¹², O. Stenyakin³⁷, M. Stepanova³¹, H. Stevens¹⁰, S. Stone⁶¹, B. Storaci⁴², S. Stracka^{24,p}, M.E. Stramaglia⁴¹, M. Straticiu³⁰, U. Straumann⁴², L. Sun⁶⁴, W. Sutcliffe⁵⁵, K. Swientek²⁸, V. Syropoulos⁴⁴, M. Szczekowski²⁹, T. Szumlak²⁸, M. Szymanski⁶³, S. T'Jampens⁴, A. Tayduganov⁶, T. Tekampe¹⁰, G. Tellarini^{17,g}, F. Teubert⁴⁰, E. Thomas⁴⁰, J. van Tilburg⁴³, M.J. Tilley⁵⁵, V. Tisserand⁴, M. Tobin⁴¹, S. Tolk⁴⁹, L. Tomassetti^{17,g}, D. Tonelli²⁴, F. Toriello⁶¹, R. Tourinho Jadallah Aoude¹, E. Tournefier⁴, M. Traill⁵³, M.T. Tran⁴¹, M. Tresch⁴², A. Trisovic⁴⁰, A. Tsaregorodtsev⁶, P. Tsopelas⁴³, A. Tully⁴⁹, N. Tuning^{43,40}, A. Ukleja²⁹, A. Usachov⁷, A. Ustyuzhanin³⁵, U. Uwer¹², C. Vacca^{16,f}, A. Vagner⁶⁹, V. Vagnoni^{15,40}, A. Valassi⁴⁰, S. Valat⁴⁰, G. Valenti¹⁵, R. Vazquez Gomez¹⁹, P. Vazquez Regueiro³⁹, S. Vecchi¹⁷, M. van Veghel⁴³, J.J. Velthuis⁴⁸, M. Veltri^{18,r}, G. Veneziano⁵⁷, A. Venkateswaran⁶¹, T.A. Verlage⁹, M. Vernet⁵, M. Vesterinen⁵⁷, J.V. Viana Barbosa⁴⁰, B. Viaud⁷, D. Vieira⁶³, M. Vieites Diaz³⁹, H. Viemann⁶⁷, X. Vilasis-Cardona^{38,m}, M. Vitti⁴⁹, V. Volkov³³, A. Vollhardt⁴², B. Voneki⁴⁰, A. Vorobyev³¹, V. Vorobyev^{36,w}, C. Vob⁹, J.A. de Vries⁴³, C. Vázquez Sierra³⁹, R. Waldi⁶⁷, C. Wallace⁵⁰, R. Wallace¹³, J. Walsh²⁴, J. Wang⁶¹, D.R. Ward⁴⁹, H.M. Wark⁵⁴, N.K. Watson⁴⁷, D. Websdale⁵⁵, A. Weiden⁴², M. Whitehead⁴⁰, J. Wicht⁵⁰, G. Wilkinson^{57,40}, M. Wilkinson⁶¹, M. Williams⁵⁶, M.P. Williams⁴⁷, M. Williams⁵⁸, T. Williams⁴⁷, F.F. Wilson⁵¹, J. Wimberley⁶⁰, M. Winn⁷, J. Wishahi¹⁰, W. Wislicki²⁹, M. Witek²⁷, G. Wormser⁷, S.A. Wotton⁴⁹, K. Wraight⁵³, K. Wyllie⁴⁰, Y. Xie⁶⁵, Z. Xu⁴, Z. Yang³, Z. Yang⁶⁰, Y. Yao⁶¹, H. Yin⁶⁵, J. Yu⁶⁵, X. Yuan⁶¹, O. Yushchenko³⁷, K.A. Zarebski⁴⁷, M. Zavertyaev^{11,c}, L. Zhang³, Y. Zhang⁷, A. Zhelezov¹², Y. Zheng⁶³, X. Zhu³, V. Zhukov³³, J.B. Zonneveld⁵², S. Zucchelli¹⁵.

¹Centro Brasileiro de Pesquisas Físicas (CBPF), Rio de Janeiro, Brazil

²Universidade Federal do Rio de Janeiro (UFRJ), Rio de Janeiro, Brazil

³Center for High Energy Physics, Tsinghua University, Beijing, China

⁴LAPP, Université Savoie Mont-Blanc, CNRS/IN2P3, Annecy-Le-Vieux, France

⁵Clermont Université, Université Blaise Pascal, CNRS/IN2P3, LPC, Clermont-Ferrand, France

⁶Aix Marseille Univ, CNRS/IN2P3, CPPM, Marseille, France

⁷LAL, Université Paris-Sud, CNRS/IN2P3, Orsay, France

⁸LPNHE, Université Pierre et Marie Curie, Université Paris Diderot, CNRS/IN2P3, Paris, France

⁹I. Physikalisches Institut, RWTH Aachen University, Aachen, Germany

¹⁰Fakultät Physik, Technische Universität Dortmund, Dortmund, Germany

¹¹Max-Planck-Institut für Kernphysik (MPIK), Heidelberg, Germany

¹²Physikalisches Institut, Ruprecht-Karls-Universität Heidelberg, Heidelberg, Germany

- ¹³*School of Physics, University College Dublin, Dublin, Ireland*
- ¹⁴*Sezione INFN di Bari, Bari, Italy*
- ¹⁵*Sezione INFN di Bologna, Bologna, Italy*
- ¹⁶*Sezione INFN di Cagliari, Cagliari, Italy*
- ¹⁷*Universita e INFN, Ferrara, Ferrara, Italy*
- ¹⁸*Sezione INFN di Firenze, Firenze, Italy*
- ¹⁹*Laboratori Nazionali dell'INFN di Frascati, Frascati, Italy*
- ²⁰*Sezione INFN di Genova, Genova, Italy*
- ²¹*Universita e INFN, Milano-Bicocca, Milano, Italy*
- ²²*Sezione di Milano, Milano, Italy*
- ²³*Sezione INFN di Padova, Padova, Italy*
- ²⁴*Sezione INFN di Pisa, Pisa, Italy*
- ²⁵*Sezione INFN di Roma Tor Vergata, Roma, Italy*
- ²⁶*Sezione INFN di Roma La Sapienza, Roma, Italy*
- ²⁷*Henryk Niewodniczanski Institute of Nuclear Physics Polish Academy of Sciences, Kraków, Poland*
- ²⁸*AGH - University of Science and Technology, Faculty of Physics and Applied Computer Science, Kraków, Poland*
- ²⁹*National Center for Nuclear Research (NCBJ), Warsaw, Poland*
- ³⁰*Horia Hulubei National Institute of Physics and Nuclear Engineering, Bucharest-Magurele, Romania*
- ³¹*Petersburg Nuclear Physics Institute (PNPI), Gatchina, Russia*
- ³²*Institute of Theoretical and Experimental Physics (ITEP), Moscow, Russia*
- ³³*Institute of Nuclear Physics, Moscow State University (SINP MSU), Moscow, Russia*
- ³⁴*Institute for Nuclear Research of the Russian Academy of Sciences (INR RAN), Moscow, Russia*
- ³⁵*Yandex School of Data Analysis, Moscow, Russia*
- ³⁶*Budker Institute of Nuclear Physics (SB RAS), Novosibirsk, Russia*
- ³⁷*Institute for High Energy Physics (IHEP), Protvino, Russia*
- ³⁸*ICCUB, Universitat de Barcelona, Barcelona, Spain*
- ³⁹*Universidad de Santiago de Compostela, Santiago de Compostela, Spain*
- ⁴⁰*European Organization for Nuclear Research (CERN), Geneva, Switzerland*
- ⁴¹*Institute of Physics, Ecole Polytechnique Fédérale de Lausanne (EPFL), Lausanne, Switzerland*
- ⁴²*Physik-Institut, Universität Zürich, Zürich, Switzerland*
- ⁴³*Nikhef National Institute for Subatomic Physics, Amsterdam, The Netherlands*
- ⁴⁴*Nikhef National Institute for Subatomic Physics and VU University Amsterdam, Amsterdam, The Netherlands*
- ⁴⁵*NSC Kharkiv Institute of Physics and Technology (NSC KIPT), Kharkiv, Ukraine*
- ⁴⁶*Institute for Nuclear Research of the National Academy of Sciences (KINR), Kyiv, Ukraine*
- ⁴⁷*University of Birmingham, Birmingham, United Kingdom*
- ⁴⁸*H.H. Wills Physics Laboratory, University of Bristol, Bristol, United Kingdom*
- ⁴⁹*Cavendish Laboratory, University of Cambridge, Cambridge, United Kingdom*
- ⁵⁰*Department of Physics, University of Warwick, Coventry, United Kingdom*
- ⁵¹*STFC Rutherford Appleton Laboratory, Didcot, United Kingdom*
- ⁵²*School of Physics and Astronomy, University of Edinburgh, Edinburgh, United Kingdom*
- ⁵³*School of Physics and Astronomy, University of Glasgow, Glasgow, United Kingdom*
- ⁵⁴*Oliver Lodge Laboratory, University of Liverpool, Liverpool, United Kingdom*
- ⁵⁵*Imperial College London, London, United Kingdom*
- ⁵⁶*School of Physics and Astronomy, University of Manchester, Manchester, United Kingdom*
- ⁵⁷*Department of Physics, University of Oxford, Oxford, United Kingdom*
- ⁵⁸*Massachusetts Institute of Technology, Cambridge, MA, United States*
- ⁵⁹*University of Cincinnati, Cincinnati, OH, United States*
- ⁶⁰*University of Maryland, College Park, MD, United States*
- ⁶¹*Syracuse University, Syracuse, NY, United States*
- ⁶²*Pontifícia Universidade Católica do Rio de Janeiro (PUC-Rio), Rio de Janeiro, Brazil, associated to ²*
- ⁶³*University of Chinese Academy of Sciences, Beijing, China, associated to ³*
- ⁶⁴*School of Physics and Technology, Wuhan University, Wuhan, China, associated to ³*
- ⁶⁵*Institute of Particle Physics, Central China Normal University, Wuhan, Hubei, China, associated to ³*
- ⁶⁶*Departamento de Física, Universidad Nacional de Colombia, Bogota, Colombia, associated to ⁸*

- ⁶⁷ *Institut für Physik, Universität Rostock, Rostock, Germany, associated to* ¹²
⁶⁸ *National Research Centre Kurchatov Institute, Moscow, Russia, associated to* ³²
⁶⁹ *National Research Tomsk Polytechnic University, Tomsk, Russia, associated to* ³²
⁷⁰ *Instituto de Fisica Corpuscular, Centro Mixto Universidad de Valencia - CSIC, Valencia, Spain, associated to* ³⁸
⁷¹ *Van Swinderen Institute, University of Groningen, Groningen, The Netherlands, associated to* ⁴³

- ^a *Universidade Federal do Triângulo Mineiro (UFTM), Uberaba-MG, Brazil*
^b *Laboratoire Leprince-Ringuet, Palaiseau, France*
^c *P.N. Lebedev Physical Institute, Russian Academy of Science (LPI RAS), Moscow, Russia*
^d *Università di Bari, Bari, Italy*
^e *Università di Bologna, Bologna, Italy*
^f *Università di Cagliari, Cagliari, Italy*
^g *Università di Ferrara, Ferrara, Italy*
^h *Università di Genova, Genova, Italy*
ⁱ *Università di Milano Bicocca, Milano, Italy*
^j *Università di Roma Tor Vergata, Roma, Italy*
^k *Università di Roma La Sapienza, Roma, Italy*
^l *AGH - University of Science and Technology, Faculty of Computer Science, Electronics and Telecommunications, Kraków, Poland*
^m *LIFAELS, La Salle, Universitat Ramon Llull, Barcelona, Spain*
ⁿ *Hanoi University of Science, Hanoi, Viet Nam*
^o *Università di Padova, Padova, Italy*
^p *Università di Pisa, Pisa, Italy*
^q *Università degli Studi di Milano, Milano, Italy*
^r *Università di Urbino, Urbino, Italy*
^s *Università della Basilicata, Potenza, Italy*
^t *Scuola Normale Superiore, Pisa, Italy*
^u *Università di Modena e Reggio Emilia, Modena, Italy*
^v *Iligan Institute of Technology (IIT), Iligan, Philippines*
^w *Novosibirsk State University, Novosibirsk, Russia*
[†] *Deceased*